

Robust Transmit Beamforming for Secure Integrated Sensing and Communication

Zixiang Ren, Ling Qiu, Jie Xu, and Derrick Wing Kwan Ng

Abstract

This paper studies a downlink secure integrated sensing and communication (ISAC) system, in which a multi-antenna base station (BS) transmits confidential messages to a single-antenna communication user (CU) while performing sensing on targets that may act as suspicious eavesdroppers. To ensure the quality of target sensing while preventing their potential eavesdropping, the BS combines the transmit confidential information signals with additional dedicated sensing signals, which play a dual role of artificial noise (AN) for degrading the qualities of eavesdropping channels. Under this setup, we jointly design the transmit information and sensing beamforming, with the objective of minimizing the weighted sum of beampattern matching errors and cross-correlation patterns for sensing subject to secure communication constraints. The robust design takes into account the channel state information (CSI) imperfectness of the eavesdroppers in two practical CSI error scenarios. First, we consider the scenario with bounded CSI errors of eavesdroppers, in which the worst-case secrecy rate constraint is adopted to ensure secure communication performance. In this scenario, we present the optimal solution to the worst-case secrecy rate constrained sensing beampattern optimization problem, by adopting the techniques of S-procedure, semi-definite relaxation (SDR), and a one-dimensional (1D) search, for which the tightness of the SDR is rigorously proved. Next, we consider the scenario with Gaussian CSI errors of eavesdroppers, in which the secrecy outage probability constraint is adopted. In this scenario, we present an efficient algorithm to solve the more challenging secrecy outage-constrained

Part of this paper has been presented at the IEEE International Conference on Communications (ICC), Seoul, South Korea, 16-20 May 2022 [1].

Z. Ren is with Key Laboratory of Wireless-Optical Communications, Chinese Academy of Sciences, School of Information Science and Technology, University of Science and Technology of China, Hefei 230027, China, and the School of Science and Engineering (SSE) and the Future Network of Intelligence Institute (FNii), The Chinese University of Hong Kong (Shenzhen), Shenzhen 518172, China (e-mail: rzx66@mail.ustc.edu.cn).

L. Qiu is with Key Laboratory of Wireless-Optical Communications, Chinese Academy of Sciences, School of Information Science and Technology, University of Science and Technology of China, Hefei 230027, China, (e-mail: lqiu@ustc.edu.cn).

J. Xu is with the SSE and the FNii, The Chinese University of Hong Kong (Shenzhen), Shenzhen 518172, China (e-mail: xujie@cuhk.edu.cn).

D. W. K. Ng is with the University of New South Wales, Sydney, NSW 2052, Australia (e-mail: w.k.ng@unsw.edu.au).

L. Qiu and J. Xu are the corresponding authors.

sensing beampattern optimization problem, by exploiting the convex restriction technique based on the Bernstein-type inequality, together with the SDR and 1D search. Finally, numerical results show that the proposed designs can properly adjust the information and sensing beams to balance the tradeoffs among communicating with CU, sensing targets, and confusing eavesdroppers, so as to achieve desirable sensing transmit beampatterns while ensuring the CU's secrecy requirements for the two scenarios.

Index Terms

Integrated sensing and communication (ISAC), physical layer security, artificial noise (AN), transmit beamforming, secrecy rate, optimization.

I. INTRODUCTION

Integrated sensing and communication (ISAC) has been widely recognized as one of the key technologies to realize future beyond fifth-generation (B5G) and sixth-generation (6G) wireless networks [2]–[4], in which sensing is integrated as new functionality to enable environment-aware intelligent applications, such as autonomous driving, industrial automation, and unmanned aerial vehicles (UAVs) [5]. Different from conventional wireless sensing and communication systems that are separately designed to compete with each other on spectrum, energy, and hardware resources, ISAC unifies the two functionalities into a joint design to exploit their mutual benefit via seamless collaboration [4]. By allowing the dual use of wireless infrastructures and scarce spectrum/power resources for performing communication and sensing simultaneously, ISAC is expected to achieve enhanced sensing and communication performance at a reduced cost.

Various research efforts have been devoted in the recent literature to unleash the ISAC potential from different aspects, such as multi-antenna beamforming [6], [7], waveform design [8], and resource allocation [4], [9]. Among others, multi-antenna beamforming is particularly appealing, in which multiple signal-carrying beams can be steered towards both the desired communication users (CUs) and sensing targets for simultaneous multi-user communications and multi-target radar sensing over the same frequency band. For instance, the authors in [8] proposed to reuse the multiple users' information signals for radar sensing, in which the transmit multi-user information beamforming vectors are optimized to minimize the inter-user interference at the CUs, while ensuring the beampattern requirements for multi-target sensing. However, when the number of CUs is less than that of transmit antennas, the exploitation of information beams only may lead to sensing beampattern distortion, due to the limited total degrees-of-freedom (DoF) utilized in

the information beams. To resolve this issue, the authors in [6], [7] proposed to additionally send the dedicated sensing signal beams together with the information beams such that the full spatial DoF can be exploited for multi-target radar sensing. In particular, the information and sensing beams were jointly optimized in [6], [7] to achieve desired transmit beampattern for radar sensing, while ensuring the individual signal-to-interference-plus-noise ratio (SINR) constraints at the CUs.

Recently, security has become increasingly important for wireless networks due to the inherent broadcast natures, while the emergence of ISAC introduces new communication security issues. In particular, as the information-bearing signals are reused for radar sensing, the optimized transmit information beams in ISAC would be steered towards sensing targets to ensure sensing performance. This, however, may lead to potential information leakage issues, as in practice the sensing targets can be suspicious eavesdroppers (e.g., suspicious UAV targets) that may try to intercept the messages sent from the ISAC transmitter [10]–[12]. To deal with the new security concern in ISAC, physical layer security has emerged as a viable solution to prevent potential eavesdropping from the sensing targets. Different from conventional cryptography-based security technologies, physical layer security aims to provide perfectly secure data delivery from the information-theoretic perspective, by exploiting the difference in physical properties between the legitimate communication channels and the eavesdropping channels (e.g., noise, interference, and fading). In practice, the secrecy rate and secrecy capacity have been employed as key performance metrics in physical layer security [13]–[15]. Specifically, the secrecy capacity is defined as the difference between the capacity of the legitimate channels and that of the eavesdropping channels, which indicates the maximum achievable data rate that can be securely transmitted over the wireless channels, provided that the eavesdroppers cannot intercept any information [16]. To enhance the secrecy performance, artificial noise (AN) has emerged as a promising technique in physical layer security [17], in which the transmitters can inject AN superimposing with the confidential information concurrently for protecting the confidential message transmission via confusing the eavesdroppers. Furthermore, in secure ISAC systems, AN can also be exploited as sensing signals, with a dual role of jamming the eavesdroppers and sensing the targets. As such, the interplay between ISAC and physical layer security enables a multi-function wireless network integrating sensing, communication, and security [12].

In general, the availability of channel state information (CSI) at the transmitter is crucial for the implementation of physical layer security and multi-antenna transmit beamforming [17],

[18]. Conventionally, to obtain the CSI of a CU, the transmitter can either exploit the CU's forward-link channel estimation and feedback in frequency division duplex (FDD) systems, or perform the reverse-link channel estimation based on the channel reciprocity in time division duplex (TDD) systems. To acquire the CSI of eavesdroppers, the transmitter may overhear their emitted radio signals for channel estimation if the eavesdroppers are active in transmission. In general, however, it is more difficult to obtain accurate CSI of eavesdroppers. As such, how to jointly design the transmission of both information and AN/sensing signals in the case of the imperfect CSI of eavesdroppers is an interesting problem in secure ISAC systems.

There have been a handful of prior works investigating the secrecy issue in ISAC systems. For instance, the authors in [10] studied the secure ISAC system with one CU and one eavesdropping target. By considering the perfect CSI at the transmitter, the transmit covariance matrices of both information signals and AN were jointly optimized to maximize the CU's secrecy rate while ensuring the received SINR requirement for sensing. Also, the authors in [11] considered the secure ISAC system with multiple CUs and one eavesdropping target by assuming line-of-sight (LoS) eavesdropping channels. For both scenarios with perfect and imperfect CSI, the signal-to-noise ratio (SNR) at the eavesdropping target was minimized in [11] while ensuring the CUs' individual SINR and certain sensing beampattern requirements. However, due to the non-convexity of the formulated problems, only sub-optimal beamforming/precoding designs were obtained in these prior works [10], [11] under their respective setups. More importantly, these prior works [10], [11] on secure ISAC with single target sensing only adopted the beampattern matching mean squared error (MSE) as the sensing performance metric but ignored the impacts of cross-correlation patterns for multi-target sensing that are shown to be important [6], [19].

This paper studies a secure ISAC system with a multi-antenna base station (BS), a single-antenna CU, and multiple sensing targets, in which a portion of targets are untrusted (acting as suspicious eavesdroppers) and the remaining are trusted. Different from prior works, e.g., [10], [11], we consider the weighted sum of the beampattern matching MSE and cross correlation patterns as the sensing performance measure. We consider that the BS sends one confidential information signal beam and multiple dedicated sensing signal beams that also play the AN role. It is assumed that the BS has the perfect CSI of the CU but imperfect CSI of the potential eavesdroppers subject to two different types of errors, namely the bounded and Gaussian errors, respectively. For these two scenarios, we jointly optimize the transmit information and sensing beamforming vectors to minimize the weighted sum of the beampattern matching error and

cross-correlation patterns for sensing, while ensuring the secure communication requirements. The main results are listed as follows.

- First, we consider the scenario with bounded CSI errors of the eavesdroppers, in which the minimum worst-case secrecy rate requirement is adopted at the CU to ensure secrecy performance. In this scenario, the worst-case secrecy rate-constrained sensing beampattern optimization problem is non-convex and thus difficult to solve in general. Fortunately, we obtain the optimal solution to this problem via the techniques of S-procedure, semi-definite relaxation (SDR), and a one-dimensional (1D) search. In particular, we rigorously prove the tightness of SDR, based on which the optimal solution with rank-one information beamforming and general-rank sensing beamforming can always be obtained via the proposed construction approach.
- Next, we consider the scenario with Gaussian CSI errors of the eavesdroppers. In this scenario, a maximum secrecy outage probability constraint is imposed to ensure secure communication performance such that the likelihood of the achievable secrecy rate being less than a required level is small. The secrecy outage-constrained sensing beampattern optimization problem, however, is more difficult to solve compared with the worst-case counterpart, as the maximum secrecy outage constraint does not admit a closed-form expression with respect to the transmit beamforming vectors. To solve this problem, we first apply the convex restriction technique based on the Bernstein-type inequality (BTI) to approximate the original problem. Then, we solve the restricted approximate problem via the SDR and 1D search, and finally propose an efficient construction method to find the desired solution to the original problem with rank-one information and general-rank sensing beamformers.
- Finally, we provide numerical results to validate the effectiveness of our proposed joint beamforming designs for the two scenarios with imperfect CSI of eavesdroppers. It is shown that in our proposed solution, the information beams are designed toward the CU and the trusted targets, and the sensing/AN beams are designed toward both untrusted and trusted targets, thus maximizing the sensing performance while ensuring the CU's secure communication requirement. It is also shown that as compared to a conventional benchmarks, our proposed joint beamforming design achieves better sensing performance in terms of lower beampattern matching errors and higher accuracy for angle estimation (by considering the practical Capon estimation algorithm [19], [20] at the sensing receiver).

We also illustrate the impacts of CSI errors on the ISAC performance. It is shown that our proposed designs are robust to the CSI errors of eavesdroppers.

The remainder of this paper is organized as follows. Section II introduces the system model and formulates the secrecy constrained sensing beampattern optimization problems for the two scenarios with bounded and Gaussian CSI errors of eavesdroppers. Sections III and IV develop efficient algorithms for solving the two problems in the two scenarios, respectively. Section V presents numerical results and Section VI concludes this paper.

Notations: Throughout this paper, vectors and matrices are denoted by bold lower- and upper-case letters, respectively. $\mathbb{C}^{N \times M}$ denotes the space of $N \times M$ matrices with complex entries. \mathbb{S}^N denotes the space of $N \times N$ Hermitian matrices, \mathbb{S}_+^N denotes the space of $N \times N$ positive semi-definite matrices, and \mathbb{S}_{++}^N denotes the space of $N \times N$ positive definite matrices. \mathbf{I} and $\mathbf{0}$ represent an identity matrix and an all-zero vector/matrix with appropriate dimensions, respectively. For a complex-valued element a , $\text{Re}(a)$ and $\text{Im}(a)$ denote its real part and imaginary part, respectively. For a square matrix \mathbf{A} , $\text{Tr}(\mathbf{A})$ denotes its trace and $\mathbf{A} \succeq \mathbf{0}$ means that \mathbf{A} is positive semi-definite. For a complex arbitrary-size matrix \mathbf{B} , $\text{rank}(\mathbf{B})$, \mathbf{B}^T , \mathbf{B}^H , and \mathbf{B}^c denote its rank, transpose, conjugate transpose, and complex conjugate, respectively. $\mathbb{E}(\cdot)$ denotes the stochastic expectation, $\|\cdot\|$ denotes the Euclidean norm of a vector, and $\mathcal{CN}(\mathbf{x}, \mathbf{Y})$ denotes the circularly symmetric complex Gaussian (CSCG) random distribution with mean vector \mathbf{x} and covariance matrix \mathbf{Y} . $(x)^+ \triangleq \max(x, 0)$.

II. SYSTEM MODEL AND PROBLEM FORMULATION

A. Signal Model

We consider a secure ISAC system as shown in Fig. 1, which consists of a BS equipped with a uniform linear array (ULA) with $N > 1$ antenna elements, a CU with a single antenna¹, and K sensing targets. Let $\mathcal{K} \triangleq \{1, \dots, K\}$ denote the set of targets, among which the first K_E ones (with $K_E \leq K$) are assumed to be untrusted or suspicious eavesdroppers, denoted by set $\mathcal{K}_E \triangleq \{1, \dots, K_E\} \subseteq \mathcal{K}$, and the remaining $K - K_E$ targets are assumed to be trusted ones. We consider that the BS adopts the linear transmit beamforming to send the confidential message $s_0(n) \in \mathbb{C}$ to the CU, where $s_0(n) \in \mathbb{C}$ is a CSCG random variable with zero mean and

¹Our proposed design principles can be extended to the case with multiple CUs each with multiple antennas, by accordingly modifying the secrecy rate formulas.

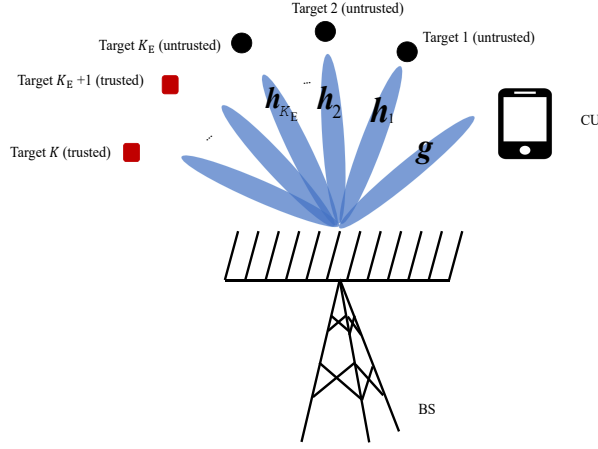


Fig. 1: Illustration of the secure ISAC system with both the trusted and untrusted targets.

unit variance, i.e., $s_0(n) \sim \mathcal{CN}(0, 1)$, with $n \in \{1, \dots, L\}$ denoting the symbol index. We use $\mathbf{w}_0 \in \mathbb{C}^{N \times 1}$ to denote the corresponding transmit information beamforming vector. Besides the information signal $s_0(n)$, the BS also sends a dedicated sensing signal or AN, denoted by vector $\mathbf{s}_1(n) \in \mathbb{C}^{N \times 1}$, to facilitate the target sensing and to confuse the eavesdropping targets. Here, $\mathbf{s}_1(n)$ is independent from $s_0(n)$ and is a CSCG random vector with zero mean and covariance matrix $\mathbf{S} = \mathbb{E}(\mathbf{s}_1(n)\mathbf{s}_1^H(n)) \succeq \mathbf{0}$, i.e., $\mathbf{s}_1(n) \sim \mathcal{CN}(\mathbf{0}, \mathbf{S})$. We assume that $s_0(n)$ and $\mathbf{s}_1(n)$ are independent over different symbols, $\forall n \in \{1, \dots, L\}$. Note that \mathbf{S} is assumed to be of a general rank with $0 \leq m = \text{rank}(\mathbf{S}) \leq N$. This corresponds to the case with m linearly and statistically independent sensing beams, each of which can be obtained via the eigenvalue decomposition (EVD) of \mathbf{S} [18]. As a result, the transmitted signal by the BS, $\mathbf{x}(n) \in \mathbb{C}^{N \times 1}$, is expressed as

$$\mathbf{x}(n) = \mathbf{w}_0 s_0(n) + \mathbf{s}_1(n). \quad (1)$$

Accordingly, the covariance matrix of $\mathbf{x}(n)$ is denoted as

$$\mathbf{T} = \mathbb{E}(\mathbf{x}(n)\mathbf{x}^H(n)) = \mathbf{W} + \mathbf{S}, \quad (2)$$

where $\mathbf{W} = \mathbf{w}_0\mathbf{w}_0^H$ with $\mathbf{W} \succeq \mathbf{0}$ and $\text{rank}(\mathbf{W}) \leq 1$. We consider that the BS is subject to the per-antenna transmit power constraints, i.e., each antenna at the BS is subject to the maximum transmit power budget Q . We define $\mathbf{E}_i \in \mathbb{C}^{N \times N}$ as a zero matrix except the i -th diagonal element being 1. In this case, we have

$$\text{Tr}(\mathbf{E}_i\mathbf{T}) = \text{Tr}(\mathbf{E}_i(\mathbf{W} + \mathbf{S})) = Q, \forall i \in \{1, \dots, N\}, \quad (3)$$

in which the full power transmission is adopted at each transmit antenna of the BS to maximize the sensing performance. Similar per-antenna full power transmission has been widely considered in the MIMO radar literature [19], [21].

B. Secure Communication

Then, we consider the secure communication model. We consider a quasi-static channel model, in which the wireless channels remain static over the time block of our interest, but may change from one block to another [6], [11]. Let $\mathbf{g} \in \mathbb{C}^{N \times 1}$ denote the channel vector from the BS to the CU. Accordingly, the received signal at the CU is expressed as

$$r_0(n) = \mathbf{g}^H \mathbf{w}_0 s_0(n) + \mathbf{g}^H \mathbf{s}_1(n) + z_0(n), \quad (4)$$

where $z_0(n) \sim \mathcal{CN}(0, \sigma_0^2)$ denotes the additive white Gaussian noise (AWGN) at the CU receiver and σ_0^2 denotes the corresponding noise power. Based on (4), the received SINR at the CU is

$$\gamma_0(\mathbf{W}, \mathbf{S}, \mathbf{g}) = \frac{\mathbf{g}^H \mathbf{W} \mathbf{g}}{\mathbf{g}^H \mathbf{S} \mathbf{g} + \sigma_0^2}. \quad (5)$$

Furthermore, by letting $\mathbf{h}_k \in \mathbb{C}^{N \times 1}$ denote the channel vector from the BS to untrusted target $k \in \mathcal{K}_E$, the received signal at untrusted target $k \in \mathcal{K}_E$ is denoted as

$$r_k(n) = \mathbf{h}_k^H \mathbf{w}_0 s_0(n) + \mathbf{h}_k^H \mathbf{s}_1(n) + z_k(n), \quad (6)$$

where $z_k(n) \sim \mathcal{CN}(0, \sigma_k^2)$ denotes the AWGN at the receiver of untrusted target $k \in \mathcal{K}_E$ and σ_k^2 denotes the corresponding noise power. Thus, the SINR at untrusted target $k \in \mathcal{K}_E$ is

$$\gamma_k(\mathbf{W}, \mathbf{S}, \mathbf{h}_k) = \frac{\mathbf{h}_k^H \mathbf{W} \mathbf{h}_k}{\mathbf{h}_k^H \mathbf{S} \mathbf{h}_k + \sigma_k^2}. \quad (7)$$

As such, under given \mathbf{g} and $\{\mathbf{h}_k\}$, the achievable secrecy rate at the CU (in bits-per-second-per-Hertz, bps/Hz) is given by [14]

$$R(\mathbf{W}, \mathbf{S}) = \min_{k \in \mathcal{K}_E} \left(\log_2 (1 + \gamma_0(\mathbf{W}, \mathbf{S}, \mathbf{g})) - \log_2 (1 + \gamma_k(\mathbf{W}, \mathbf{S}, \mathbf{h}_k)) \right)^+. \quad (8)$$

It is assumed that the BS has perfect CSI of the CU but imperfect CSI of the eavesdroppers. Let $\hat{\mathbf{h}}_k$ denote the estimated CSI of eavesdropping target $k \in \mathcal{K}_E$ at the BS. The CSI estimation error vector of eavesdropping target $k \in \mathcal{K}_E$ is expressed as

$$\mathbf{e}_k = \mathbf{h}_k - \hat{\mathbf{h}}_k, \forall k \in \mathcal{K}_E. \quad (9)$$

It is assumed that the error vector \mathbf{e}_k is independent from $\hat{\mathbf{h}}_k$, $\forall k \in \mathcal{K}_E$. In particular, we consider two practical scenarios with bounded and Gaussian CSI errors for $\{\mathbf{e}_k\}$, respectively.

1) *Bounded CSI Errors*: In the first scenario, the CSI of each eavesdropper is subject to a bounded error, i.e.,

$$\|\mathbf{e}_k\| \leq \varepsilon_k, \forall k \in \mathcal{K}_E, \quad (10)$$

where ε_k denotes the maximum threshold of the bounded CSI error. Under given \mathbf{g} and distribution of $\{\mathbf{h}_k\}$, the *worst-case* secrecy rate [22] is employed as the secure communication metric in this scenario, i.e.,

$$R_w(\mathbf{W}, \mathbf{S}) = \min_{k \in \mathcal{K}_E} \left(\log_2 (1 + \gamma_0(\mathbf{W}, \mathbf{S}, \mathbf{g})) - \max_{\|\mathbf{e}_k\| \leq \varepsilon_k} \log_2 (1 + \gamma_k(\mathbf{W}, \mathbf{S}, \mathbf{h}_k)) \right)^+. \quad (11)$$

2) *Gaussian CSI Errors*: In the second scenario, the CSI of the eavesdroppers is subject to Gaussian errors, i.e., $\mathbf{e}_k \sim \mathcal{CN}(\mathbf{0}, \mathbf{C}_k)$, $\forall k \in \mathcal{K}_E$, where $\mathbf{C}_k \in \mathbb{S}_+^N$ denotes the covariance matrix of CSI error for eavesdropping target $k \in \mathcal{K}_E$. For notational convenience, we express (9) as

$$\mathbf{h}_k = \hat{\mathbf{h}}_k + \mathbf{C}_k^{\frac{1}{2}} \mathbf{u}_k, \forall k \in \mathcal{K}_E, \quad (12)$$

where \mathbf{u}_k denotes independent CSCG random vectors with mean zero and variance \mathbf{I} , i.e., $\mathbf{u}_k \sim \mathcal{CN}(\mathbf{0}, \mathbf{I})$. It is assumed that \mathbf{u}_k is independent over different $k \in \mathcal{K}_E$. Thus, \mathbf{h}_k is independent of \mathbf{h}_l , for any $k, l \in \mathcal{K}_E, k \neq l$ [23]. With given \mathbf{g} and the Gaussian CSI error model in (12), we adopt the secrecy outage probability as the secure communication performance measure, which is defined as the probability of the achievable secrecy rate in (8) being lower than a given threshold R_0 , i.e.,

$$\Pr(R(\mathbf{W}, \mathbf{S}) < R_0). \quad (13)$$

In (13), the probability is taken over the randomness of $\{\mathbf{u}_k\}$ based on (12).

C. Radar Sensing

Next, we consider the monostatic radar sensing at the BS [6], [19]. As the BS has the complete knowledge of the transmitted information waveform, the information message $s_0(n)$ can be exploited together with the dedicated sensing signal $\mathbf{s}_1(n)$ for target sensing. We assume that the targets are in the far-field region, each of which can be viewed as a point target with angle $\theta_k, k \in \mathcal{K}$. In this case, supposing that the BS is equipped with the same number of N antennas for signal reception, the received echo signal $\mathbf{y}(n) \in \mathbb{C}^{N \times 1}$ at the BS is denoted as [19]

$$\mathbf{y}(n) = \sum_{k=1}^K \beta_k \mathbf{a}^c(\theta_k) \mathbf{a}^H(\theta_k) \mathbf{x}(n) + \mathbf{z}(n), \quad (14)$$

where $\beta_k \in \mathbb{C}$ denotes the complex round-trip channel coefficient of target $k \in \mathcal{K}$ depending on the associated path loss and its radar cross section (RCS), $\mathbf{z}(n) \in \mathbb{C}^{N \times 1}$ denotes the background noise at the BS receiver (including clutters or interference), and $\mathbf{a}(\theta)$ denotes the steering vector with an angle θ , i.e.,

$$\mathbf{a}(\theta) = [1, e^{j2\pi \frac{d}{\lambda} \sin(\theta)}, \dots, e^{j2\pi(N-1) \frac{d}{\lambda} \sin(\theta)}]^T. \quad (15)$$

In (15), λ denotes the carrier wavelength and d denotes the spacing between two adjacent antennas at the BS.

We consider the tracking task with the objective of estimating $\{\theta_k\}$ of the K targets based on (15), in which the BS *a priori* knows the number of targets K and their initial angle estimation $\{\hat{\theta}_k\}$ (e.g., based on the preceding detection) [24]. To facilitate sensing design, for any sensing angle $\theta \in [-\frac{\pi}{2}, \frac{\pi}{2}]$, we define the beampattern gain $P(\theta)$ as the transmit signal power distribution at that angle [19], [24], i.e.,

$$P(\theta) = \mathbb{E} \left(\left| \mathbf{a}^H(\theta)(\mathbf{s}_1 + \mathbf{w}_0 s_0) \right|^2 \right) = \mathbf{a}^H(\theta)(\mathbf{W} + \mathbf{S})\mathbf{a}(\theta). \quad (16)$$

For any two sensing angle $\hat{\theta}_p$ and $\hat{\theta}_q$ ($p, q \in \mathcal{K}, p \neq q$), we define the cross-correlation pattern as $\mathbf{a}^H(\hat{\theta}_p)\mathbf{T}\mathbf{a}(\hat{\theta}_q)$.

In order to optimize the sensing performance for estimation, the transmitted beampattern should be designed to satisfy the following two requirements [19].

- First, we need to control the transmit beampattern $\{P(\theta)\}$ to mimic a desired transmit beampattern $\hat{P}(\theta)$ as follows based on the estimated directions $\{\hat{\theta}_k\}$, [6], [11], [21], [24],

$$\hat{P}(\theta) = \begin{cases} 1 & \exists k \in \mathcal{K}, |\theta - \hat{\theta}_k| < \frac{\Delta\theta}{2}, \\ 0 & \text{otherwise,} \end{cases} \quad (17)$$

where $\Delta\theta$ denotes the width of desired beampattern at each estimation angle. Towards this end, we adopt the beampattern matching mean squared error (MSE), $B(\{\bar{\theta}_m\}_{m=1}^M, \mathbf{S}, \mathbf{W}, \eta)$, as the performance metric for quantifying the quality of beampattern matching, which measures the difference between the actual transmit beampattern $\{P(\theta)\}$ in the angular domain versus the desired beampattern $\{\hat{P}(\theta)\}$, i.e.,

$$B(\{\bar{\theta}_m\}_{m=1}^M, \mathbf{S}, \mathbf{W}, \eta) = \frac{1}{M} \sum_{m=1}^M \left| \eta \hat{P}(\bar{\theta}_m) - \mathbf{a}^H(\bar{\theta}_m)(\mathbf{W} + \mathbf{S})\mathbf{a}(\bar{\theta}_m) \right|^2. \quad (18)$$

In (18), $\{\bar{\theta}_m\}_{m=1}^M$ denote the M sample angles over $[-\frac{\pi}{2}, \frac{\pi}{2}]$ and η is a scaling factor to be optimized.

- Next, we need to minimize the cross-correlation $|\mathbf{a}^H(\hat{\theta}_p)\mathbf{T}\mathbf{a}(\hat{\theta}_q)|$ at $\hat{\theta}_p$ and $\hat{\theta}_q$, for any $p, q \in \mathcal{K}, p \neq q$ to resolve different target angles efficiently. Towards this end, we use the mean squared value at different estimated target directions $C(\{\hat{\theta}_k\}, \mathbf{S}, \mathbf{W})$ as the performance metric [6], [24], i.e.,

$$C(\{\hat{\theta}_k\}, \mathbf{S}, \mathbf{W}) = \frac{2}{K^2 - K} \sum_{p=1}^K \sum_{q=p+1}^K \left| \mathbf{a}^H(\hat{\theta}_p)(\mathbf{W} + \mathbf{S})\mathbf{a}(\hat{\theta}_q) \right|^2. \quad (19)$$

To capture the importance of $B(\{\bar{\theta}_m\}_{m=1}^M, \mathbf{S}, \mathbf{W}, \eta)$ in (18) and $C(\{\hat{\theta}_k\}, \mathbf{S}, \mathbf{W})$ in (19), we adopt the weighted sum of beampattern matching MSE and cross-correlation pattern in the following as the sensing performance metric to be minimized, similarly as that in [19]:

$$\begin{aligned}
D(\mathbf{S}, \mathbf{W}, \eta) &= \frac{1}{M} \sum_{m=1}^M \left| \eta \hat{P}(\bar{\theta}_m) - \mathbf{a}^H(\bar{\theta}_m)(\mathbf{W} + \mathbf{S})\mathbf{a}(\bar{\theta}_m) \right|^2 \\
&\quad + \frac{2\omega_C}{K^2 - K} \sum_{p=1}^K \sum_{q=p+1}^K \left| \mathbf{a}^H(\hat{\theta}_p)(\mathbf{W} + \mathbf{S})\mathbf{a}(\hat{\theta}_q) \right|^2, \tag{20}
\end{aligned}$$

where $\omega_C \geq 0$ is the weight of the cross-correlation term that is pre-determined. As shown in [19] for MIMO radar sensing, by designing \mathbf{W} and \mathbf{S} to properly optimize the weighted sum in (20), the multi-target estimation performance can be efficiently optimized.²

D. Problem Formulation

Our objective is to minimize the weighted sum of beampattern matching MSE and cross-correlation patterns $D(\mathbf{S}, \mathbf{W}, \eta)$ in (20), by jointly optimizing the transmit information covariance matrix \mathbf{W} and the sensing/AN covariance matrix \mathbf{S} , subject to the secure communication requirements under two scenarios with different CSI error models of eavesdroppers.

First, we consider the scenario with the bounded CSI errors of eavesdroppers. In this scenario, the worst-case secrecy rate in (13) is adopted as the performance metric. The worst-case secrecy rate constrained beampattern optimization problem is formulated as

$$\begin{aligned}
\text{(P1)} : \quad & \min_{\mathbf{W}, \mathbf{S}, \eta} D(\mathbf{W}, \mathbf{S}, \eta) \\
\text{s.t.} \quad & R_w(\mathbf{W}, \mathbf{S}) \geq R_0, \tag{21a}
\end{aligned}$$

$$\text{Tr}(\mathbf{E}_i(\mathbf{W} + \mathbf{S})) = Q, \forall i \in \{1, \dots, N\}, \tag{21b}$$

$$\mathbf{W} \succeq \mathbf{0}, \mathbf{S} \succeq \mathbf{0}, \tag{21c}$$

$$\text{rank}(\mathbf{W}) \leq 1, \tag{21d}$$

where R_0 denotes the constant worst-case secrecy rate threshold required at the CU. Notice that problem (P1) is non-convex due to the non-convex worst-case secrecy rate constraint (21a) and the rank constraint (21d), and thus is difficult to solve. Despite the difficulty, we will optimally solve problem (P1) in Section III.

Next, we consider the Gaussian CSI errors of eavesdroppers. In this scenario, we need to ensure the secrecy outage probability $\Pr(R(\mathbf{W}, \mathbf{S}) < R_0)$ in (11) not to exceed a certain threshold ρ to satisfy the secure communication performance. The secrecy outage-constrained beampattern optimization problem is formulated as

²The multi-target estimation performance in secure ISAC of our interest will be shown in Section V using the practical Capon estimation algorithm [19], [20], [24].

$$\begin{aligned}
\text{(P2): } & \min_{\mathbf{W}, \mathbf{S}, \eta} D(\mathbf{W}, \mathbf{S}, \eta) \\
& \text{s.t. } \Pr(R(\mathbf{W}, \mathbf{S}) < R_0) \leq \rho,
\end{aligned} \tag{22a}$$

$$\text{Tr}(\mathbf{E}_i(\mathbf{W} + \mathbf{S})) = Q, \forall i \in \{1, \dots, N\}, \tag{22b}$$

$$\mathbf{W} \succeq \mathbf{0}, \mathbf{S} \succeq \mathbf{0}, \tag{22c}$$

$$\text{rank}(\mathbf{W}) \leq 1, \tag{22d}$$

where $0 < \rho < 0.5$ is the given outage threshold. In problem (P2), the rank constraint in (22d) is non-convex and the secrecy outage constraint in (22a) even does not admit a closed-form expression. Therefore, problem (P2) is more difficult to solve than (P1). We will propose an efficient algorithm to solve problem (P2) in Section IV.

Remark 1. It is worth emphasizing that for the special case with perfect CSI of eavesdroppers, the simplified secrecy rate-constrained beamforming optimization problem (i.e., (P1) with $\mathbf{e}_k = \mathbf{0}$ or $\varepsilon_k = 0, \forall k \in \mathcal{K}_E$ and (P2) with $\mathbf{C}_k = \mathbf{0}, \forall k \in \mathcal{K}_E$ and $\rho = 0$) is novel and has not been addressed in the literature yet, e.g., [10], [11]. As will be shown in Section III, this simplified problem can be solved optimally based on the optimal solution to (P1). Therefore, we will not address this subcase separately. Instead, we will present numerical results for it in Section V-A to obtain more insights.

III. OPTIMAL JOINT BEAMFORMING SOLUTION TO PROBLEM (P1)

This section presents the optimal joint transmit beamforming solution to problem (P1). Towards this end, we first deal with the rank constraint in (21d) based on the idea of SDR. By dropping the rank constraint in (21d), we obtain a relaxed version of (P1) as

$$\begin{aligned}
\text{(P1.1): } & \min_{\mathbf{W}, \mathbf{S}, \eta} D(\mathbf{W}, \mathbf{S}, \eta) \\
& \text{s.t. } (21a), (21b), \text{ and } (21c).
\end{aligned}$$

In the following subsections, we first obtain the optimal solution to problem (P1.1) with general-rank information covariance \mathbf{W} . Then, we propose a construction method to find an optimal rank-one solution of \mathbf{W} for (P1).

A. Optimal Solution to (P1.1)

In the following, we focus on solving problem (P1.1) with the non-convex worst-case secrecy rate constraint (21a). First, we introduce an auxiliary optimization variable γ to represent the

SINR threshold at the CU such that the worst-case secrecy rate constraint (21a) is equivalently reformulated as

$$\frac{\mathbf{g}^H \mathbf{W} \mathbf{g}}{\mathbf{g}^H \mathbf{S} \mathbf{g} + \sigma_0^2} \geq \gamma, \max_{\|\mathbf{e}_k\| \leq \varepsilon_k} \frac{(\hat{\mathbf{h}}_k + \mathbf{e}_k)^H \mathbf{W} (\hat{\mathbf{h}}_k + \mathbf{e}_k)}{(\hat{\mathbf{h}}_k + \mathbf{e}_k)^H \mathbf{S} (\hat{\mathbf{h}}_k + \mathbf{e}_k) + \sigma_k^2} \leq \varphi(\gamma), \forall k \in \mathcal{K}_E, \quad (23)$$

where $\varphi(\gamma) = 2^{-R_0}(1 + \gamma) - 1$, and $(\cdot)^+$ in the worst-case secrecy rate formula in (21a) is omitted without loss of optimality. Notice that in order for γ to be feasible to (P1.1), it must hold that $\gamma \in \Gamma \triangleq \{\gamma | 2^{R_0} - 1 \leq \gamma \leq NQ\|\mathbf{g}\|^2/\sigma_0^2\}$. Therefore, problem (P1.1) is equivalently expressed as

$$(P1.2): \quad \min_{\mathbf{W}, \mathbf{S}, \eta, \gamma \in \Gamma} D(\mathbf{W}, \mathbf{S}, \eta) \\ \text{s.t.} \quad \mathbf{g}^H \mathbf{W} \mathbf{g} \geq \gamma(\mathbf{g}^H \mathbf{S} \mathbf{g} + \sigma_0^2), \quad (24a)$$

$$\mathbf{e}_k^H (\mathbf{W} - \varphi(\gamma) \mathbf{S}) \mathbf{e}_k + 2\text{Re} \left(\mathbf{e}_k^H (\mathbf{W} - \varphi(\gamma) \mathbf{S}) \hat{\mathbf{h}}_k \right) \\ + \hat{\mathbf{h}}_k^H (\mathbf{W} - \varphi(\gamma) \mathbf{S}) \hat{\mathbf{h}}_k - \varphi(\gamma) \sigma_k^2 \leq 0, \forall \|\mathbf{e}_k\| \leq \varepsilon_k, \forall k \in \mathcal{K}_E, \quad (24b)$$

(21b) and (21c).

Then, we introduce the S-procedure in the following lemma [25] to handle constraint (24b).

Lemma 1. *Suppose that $f_i(\mathbf{v}) = \mathbf{v}^H \mathbf{M}_i \mathbf{v} + 2\text{Re} \{ \mathbf{v}^H \mathbf{b}_i \} + n_i$, $\mathbf{M}_i \in \mathbb{S}^N$, $\mathbf{b}_i \in \mathbb{C}^{N \times 1}$, $i = 1, 2$, where there exists a point $\hat{\mathbf{v}}$ such that $f_1(\hat{\mathbf{v}}) < 0$. Then, it follows that $f_1(\mathbf{v}) \leq 0 \implies f_2(\mathbf{v}) \leq 0$ if and only if there exists $\lambda \geq 0$ such that*

$$\lambda \begin{bmatrix} \mathbf{M}_1 & \mathbf{b}_1 \\ \mathbf{b}_1^H & n_1 \end{bmatrix} - \begin{bmatrix} \mathbf{M}_2 & \mathbf{b}_2 \\ \mathbf{b}_2^H & n_2 \end{bmatrix} \succeq \mathbf{0}. \quad (25)$$

Notice that constraint (24b) is equivalent to

$$\mathbf{e}_k^H \mathbf{e}_k - \varepsilon_k^2 \leq 0 \implies \mathbf{e}_k^H (\mathbf{W} - \varphi(\gamma) \mathbf{S}) \mathbf{e}_k + 2\text{Re} \left(\mathbf{e}_k^H (\mathbf{W} - \varphi(\gamma) \mathbf{S}) \hat{\mathbf{h}}_k \right) \\ + \hat{\mathbf{h}}_k^H (\mathbf{W} - \varphi(\gamma) \mathbf{S}) \hat{\mathbf{h}}_k - \varphi(\gamma) \sigma_k^2 \leq 0, \forall k \in \mathcal{K}_E. \quad (26)$$

Therefore, based on Lemma 1, constraint (26) or equivalent (24b) is equivalently rewritten as

$$\begin{bmatrix} \lambda_k \mathbf{I} - (\mathbf{W} - \varphi(\gamma) \mathbf{S}) & -(\mathbf{W} - \varphi(\gamma) \mathbf{S}) \hat{\mathbf{h}}_k \\ -\hat{\mathbf{h}}_k^H (\mathbf{W} - \varphi(\gamma) \mathbf{S}) & -\lambda_k \varepsilon_k^2 - \hat{\mathbf{h}}_k^H (\mathbf{W} - \varphi(\gamma) \mathbf{S}) \hat{\mathbf{h}}_k + \varphi(\gamma) \sigma_k^2 \end{bmatrix} \succeq \mathbf{0}, \lambda_k \geq 0, \forall k \in \mathcal{K}_E, \quad (27)$$

where $\{\lambda_k\}$ are the new auxiliary optimization variables. Hence, problem (P1.2) can be equivalently reformulated as

$$(P1.3): \quad \min_{\mathbf{W}, \mathbf{S}, \eta, \gamma \in \Gamma, \{\lambda_k\}} D(\mathbf{W}, \mathbf{S}, \eta) \\ \text{s.t.} \quad (21b), (21c), (24a), \text{ and } (27).$$

Problem (P1.3) is still non-convex due to the non-convex constraints in (24a) and (27). To facilitate the development of solution to (P1.3), we consider the optimization of \mathbf{W} , \mathbf{S} , η , and

$\{\lambda_k\}$ in problem (P1.3) under any given $\gamma \in \Gamma$ as

$$(P1.4) : \quad \min_{\mathbf{w}, \mathbf{S}, \eta, \{\lambda_k\}} D(\mathbf{W}, \mathbf{S}, \eta)$$

$$\text{s.t.} \quad (21b), (21c), (24a), \text{ and } (27).$$

It is observed that with given γ , (24a) is an affine constraint and (27) is a linear matrix inequality (LMI) constraint, both of which are convex. Therefore, problem (P1.4) is a convex quadratic semidefinite programming (QSDP) problem that can be optimally solvable via off-the-shelf convex programming numerical solvers such as CVX [26].

Let $f(\gamma)$ denote the optimal objective value achieved by problem (P1.4) with given γ . Then we solve problem (P1.3) by first solving problem (P1.4) under any given γ and then searching over $\gamma \in \Gamma$ via a 1D search in the following problem:

$$(P1.5) : \quad \min_{\gamma \in \Gamma} f(\gamma).$$

Therefore, by optimally solving problem (P1.4) together with the 1D search for solving problem (P1.5), the optimal solution to problem (P1.3) is obtained, which is denoted as $\tilde{\mathbf{W}}^*$, $\tilde{\mathbf{S}}^*$, $\tilde{\gamma}^*$, $\tilde{\eta}^*$, and $\{\tilde{\lambda}^*\}$. Accordingly, $\tilde{\mathbf{W}}^*$, $\tilde{\mathbf{S}}^*$, and $\tilde{\eta}^*$ are the optimal solution to problem (P1.1). Notice that $\text{rank}(\tilde{\mathbf{W}}^*) \leq 1$ may not hold in general. Therefore, the obtained $\tilde{\mathbf{W}}^*$, $\tilde{\mathbf{S}}^*$, and $\tilde{\eta}^*$ from the numerical solvers may not be always feasible for problem (P1).

B. Construction of Rank-one Solution of \mathbf{W} for (P1)

To address the aforementioned issue, we propose a novel approach to construct a rank-one solution of \mathbf{W} to problem (P1) if $\text{rank}(\tilde{\mathbf{W}}^*) > 1$. In the following proposition, we construct an optimal solution to problem (P1.3) satisfying the rank-one constraint in (21d).

Proposition 1. Based on the obtained optimal solution $\tilde{\mathbf{W}}^*$, $\tilde{\mathbf{S}}^*$, $\tilde{\gamma}^*$, $\tilde{\eta}^*$, and $\{\tilde{\lambda}_k^*\}$ to problem (P1.3), we can always construct an equivalent solution of \mathbf{W}^* , \mathbf{S}^* , γ^* , η^* , and $\{\lambda_k^*\}$ in the following, which is also optimal to problem (P1.3) with $\text{rank}(\mathbf{W}^*) = 1$.

$$\mathbf{W}^* = \frac{\tilde{\mathbf{W}}^* \mathbf{g} \mathbf{g}^H \tilde{\mathbf{W}}^*}{\mathbf{g}^H \tilde{\mathbf{W}}^* \mathbf{g}}, \quad (30a)$$

$$\mathbf{S}^* = \tilde{\mathbf{W}}^* + \tilde{\mathbf{S}}^* - \mathbf{W}^*, \quad (30b)$$

$$\eta^* = \tilde{\eta}^*, \gamma^* = \tilde{\gamma}^*, \lambda_k^* = \tilde{\lambda}_k^*, \forall k \in \mathcal{K}_E. \quad (30c)$$

Proof. Please refer to Appendix A. □

Proposition 1 shows the existence of the optimal rank-one information covariance matrix to problem (P1.3) and thus (P1), which validates that the adopted SDR of problem (P1) is tight. Therefore, the constructed solution \mathbf{W}^* , \mathbf{S}^* , and η^* is optimal to problem (P1.1) with $\text{rank}(\mathbf{W}^*) = 1$ thus is also optimal to problem (P1).

IV. PROPOSED JOINT BEAMFORMING SOLUTION TO PROBLEM (P2)

In this section, we propose an efficient solution to the secrecy outage constrained sensing beampattern optimization problem (P2). Notice that the secrecy outage constraint in (22a) is equivalent to

$$\Pr(R(\mathbf{W}, \mathbf{S}) \geq R_0) \geq 1 - \rho. \quad (31)$$

By dropping the rank constraint in (22d) similarly as for problem (P1) and replacing (22a) as (31), we relax problem (P2) as

$$\begin{aligned} \text{(P2.1): } & \min_{\mathbf{W}, \mathbf{S}, \eta} D(\mathbf{W}, \mathbf{S}, \eta) \\ & \text{s.t.} \quad (22\text{b}), (22\text{c}), \text{ and } (31). \end{aligned}$$

By introducing an auxiliary optimization variable γ , the secrecy outage constraint in (31) is equivalently reformulated as

$$\frac{\mathbf{g}^H \mathbf{W} \mathbf{g}}{\mathbf{g}^H \mathbf{S} \mathbf{g} + \sigma_0^2} \geq \gamma, \quad (33)$$

$$\Pr\left(\log_2(1 + \gamma) - \max_{k \in \mathcal{K}_E} \log_2\left(1 + \frac{\mathbf{h}_k^H \mathbf{W} \mathbf{h}_k}{\mathbf{h}_k^H \mathbf{S} \mathbf{h}_k + \sigma_k^2}\right) \geq R_0\right) \geq 1 - \rho. \quad (34)$$

We denote the feasible region of γ as $\Gamma = \{\gamma | 2^{R_0} - 1 \leq \gamma \leq NQ\|\mathbf{g}\|^2/\sigma_0^2\}$. Thus, problem (P2.1) is equivalently rewritten as

$$\begin{aligned} \text{(P2.2): } & \min_{\mathbf{W}, \mathbf{S}, \eta, \gamma \in \Gamma} D(\mathbf{W}, \mathbf{S}, \eta) \\ & \text{s.t.} \quad (22\text{b}), (22\text{c}), (33), \text{ and } (34). \end{aligned}$$

To solve problem (P2.2), we consider the optimization of \mathbf{W} , \mathbf{S} , and η under given γ , which is given by

$$\begin{aligned} \text{(P2.3): } & \min_{\mathbf{W}, \mathbf{S}, \eta} D(\mathbf{W}, \mathbf{S}, \eta) \\ & \text{s.t.} \quad (22\text{b}), (22\text{c}), (33), \text{ and } (34). \end{aligned}$$

We denote the obtained objective value for problem (P2.3) as $f_2(\gamma)$. As a result, we solve problem (P2.2) equivalently by first solving (P2.3) under any given $\gamma \in \Gamma$, and then find the optimal γ that minimizes $f_2(\gamma)$ over Γ via a 1D search.

Now, we only need to focus on solving problem (P2.3) with given $\gamma \in \Gamma$. In the following, we first propose a safe decomposition for constraint (34), then exploit the convex restriction technique of BTI to establish restricted surrogate convex problems for solving (P2.3), and finally construct a high-quality solution to the original problem (P2) based on the solution to (P2.3).

A. Safe Decomposition for Constraint (34)

To solve problem (P2.3), we first deal with the secrecy outage constraint (34). Recall that \mathbf{h}_k 's are the channel vectors of different eavesdroppers that are assumed to be independent. Therefore, we have

$$\begin{aligned} & \Pr\left(\log_2(1 + \gamma) - \max_{k \in \mathcal{K}_E} \log_2\left(1 + \frac{\mathbf{h}_k^H \mathbf{W} \mathbf{h}_k}{\mathbf{h}_k^H \mathbf{S} \mathbf{h}_k + \sigma_k^2}\right) \geq R_0\right) \\ &= \prod_{k \in \mathcal{K}_E} \Pr\left(\log_2(1 + \gamma) - \log_2\left(1 + \frac{\mathbf{h}_k^H \mathbf{W} \mathbf{h}_k}{\mathbf{h}_k^H \mathbf{S} \mathbf{h}_k + \sigma_k^2}\right) \geq R_0\right). \end{aligned} \quad (36)$$

Based on (36), it follows that constraint (34) is equivalent to

$$\prod_{k \in \mathcal{K}_E} \Pr\left(\frac{\mathbf{h}_k^H \mathbf{W} \mathbf{h}_k}{\mathbf{h}_k^H \mathbf{S} \mathbf{h}_k + \sigma_k^2} \leq \varphi(\gamma)\right) \geq 1 - \rho, \quad (37)$$

where $\varphi(\gamma) = 2^{-R_0}(\gamma + 1) - 1$. However, it is still difficult to express constraint (37) into a tractable form. To resolve this issue, we replace (37) by the following K_E restricted constraints³ [23]

$$\Pr\left(\frac{\mathbf{h}_k^H \mathbf{W} \mathbf{h}_k}{\mathbf{h}_k^H \mathbf{S} \mathbf{h}_k + \sigma_k^2} \leq \varphi(\gamma)\right) \geq 1 - \bar{\rho}, \forall k \in \mathcal{K}_E, \quad (38)$$

with $\bar{\rho} = 1 - (1 - \rho)^{\frac{1}{K_E}}$, which ensure that the probability of each untrusted target's SINR being less than threshold $\varphi(\gamma)$ is less than $\bar{\rho}$.

Now, we deal with (38). Recall that $\mathbf{h}_k = \hat{\mathbf{h}}_k + \mathbf{C}_k^{\frac{1}{2}} \mathbf{u}_k, \forall k \in \mathcal{K}_E$, where $\mathbf{u}_k \sim \mathcal{CN}(\mathbf{0}, \mathbf{I})$. Accordingly, it follows that

$$\frac{\mathbf{h}_k^H \mathbf{W} \mathbf{h}_k}{\mathbf{h}_k^H \mathbf{S} \mathbf{h}_k + \sigma_k^2} \leq \varphi(\gamma) \iff \mathbf{u}_k^H \mathbf{A}_k \mathbf{u}_k + 2\text{Re}\{\mathbf{u}_k^H \mathbf{q}_k\} + c_k \geq 0, k \in \mathcal{K}_E, \quad (39)$$

where

$$\mathbf{A}_k = \mathbf{C}_k^{\frac{1}{2}} (\varphi(\gamma) \mathbf{S} - \mathbf{W}) \mathbf{C}_k^{\frac{1}{2}}, \quad (40a)$$

$$\mathbf{q}_k = \mathbf{C}_k^{\frac{1}{2}} (\varphi(\gamma) \mathbf{S} - \mathbf{W}) \hat{\mathbf{h}}_k, \quad (40b)$$

$$c_k = \hat{\mathbf{h}}_k^H (\varphi(\gamma) \mathbf{S} - \mathbf{W}) \hat{\mathbf{h}}_k + \sigma_k^2 \varphi(\gamma). \quad (40c)$$

³Note that the equivalence between (34) and (37) holds based on the assumption that \mathbf{h}_k 's are independent and the restriction from (37) to (38) does not depend on the independence of $\{\mathbf{h}_k\}$, since the feasible set of \mathbf{W} and \mathbf{S} characterized by (38) is always a subset of that by (37).

Based on (39), the constraints in (38) are equivalent to

$$\Pr\left(\mathbf{u}_k^H \mathbf{A}_k \mathbf{u}_k + 2\text{Re}\{\mathbf{u}_k^H \mathbf{q}_k\} + c_k \geq 0\right) \geq 1 - \bar{\rho}, \forall k \in \mathcal{K}_E. \quad (41)$$

By substituting (34) as (41), a restricted version of (P2.3) is obtained as

$$\begin{aligned} \text{(P2.4): } & \min_{\mathbf{W}, \mathbf{S}, \eta} D(\mathbf{W}, \mathbf{S}, \eta) \\ & \text{s.t. } \quad (22\text{b}), (22\text{c}), (33), \text{ and } (41). \end{aligned}$$

For problem (P2.4), although there is still no closed-form expression for (41), there have been some well-established approaches such as the BTI [25] to transform (41) into restricted convex constraints. In the following subsection, we solve problem (P2.4) via the convex restriction technique based on the BTI.

B. Convex Restriction of Problem (P2.4) via BTI

This subsection solves problem (P2.4) by reformulating it into a restricted problem based on the BTI in the following lemma [27].

Lemma 2. *For any $\mathbf{A} \in \mathbb{S}^n$, $\mathbf{q} \in \mathbb{C}^n$, $c \in \mathbb{R}$, $\mathbf{v} \sim \mathcal{CN}(\mathbf{0}, \mathbf{I})$, and $\rho \in (0, 1]$, if there exist a and b , such that*

$$\text{Tr}(\mathbf{A}) - \sqrt{-2\ln(\rho)} \cdot a + \ln(\rho) \cdot b + c \geq 0, \quad (42)$$

$$\left\| \begin{bmatrix} \sqrt{2}\mathbf{q} \\ \text{vec}(\mathbf{A}) \end{bmatrix} \right\| \leq a, \quad (43)$$

$$b\mathbf{I} + \mathbf{A} \succeq \mathbf{0}, \quad b \geq 0, \quad (44)$$

the following implication holds true

$$\Pr(\mathbf{v}^H \mathbf{A} \mathbf{v} + 2\text{Re}\{\mathbf{v}^H \mathbf{q}\} + c \geq 0) \geq 1 - \rho. \quad (45)$$

Based on Lemma 2, it follows that (41) can be restricted as the following set of inequalities.

$$\text{Tr}(\mathbf{A}_k) - \sqrt{-2\ln(\bar{\rho})} \cdot a_k + \ln(\bar{\rho}) \cdot b_k + c_k \geq 0, \forall k \in \mathcal{K}_E, \quad (46\text{a})$$

$$\left\| \begin{bmatrix} \sqrt{2}\mathbf{q}_k \\ \text{vec}(\mathbf{A}_k) \end{bmatrix} \right\| \leq a_k, \forall k \in \mathcal{K}_E, \quad (46\text{b})$$

$$b_k \mathbf{I} + \mathbf{A}_k \succeq \mathbf{0}, \quad b_k \geq 0, \forall k \in \mathcal{K}_E. \quad (46\text{c})$$

In other words, if (46a), (46b), and (46c) hold, then (41) is satisfied. By substituting (41) as

(46a), (46b), and (46c), we obtain a restricted version of problem (P2.4) as

$$(P2.5): \quad \min_{\mathbf{W}, \mathbf{S}, \eta, \{a_k\}, \{b_k\}} D(\mathbf{W}, \mathbf{S}, \eta)$$

$$\text{s.t.} \quad (22b), (22c), (33), (46a), (46b), \text{ and } (46c) .$$

Here, the restricted problem (P2.5) is convex and thus can be optimally solved via CVX, for which the obtained optimal solution is a high-quality solution to problem (P2.4).

So far, by solving restricted problem (P2.5), problem (P2.4) has been efficiently solved with a given $\gamma \in \Gamma$. Based on this together with the 1D search over $\gamma \in \Gamma$, an efficient solution to problem (P2.1) is also obtained, which is denoted by $\tilde{\mathbf{W}}^*$, $\tilde{\mathbf{S}}^*$, and $\tilde{\eta}^*$. However, $\tilde{\mathbf{W}}^*$ may not satisfy $\text{rank}(\tilde{\mathbf{W}}^*) \leq 1$ in general and thus the obtained solution may not be feasible to the original problem (P2).

C. Rank-one Construction of \mathbf{W} for Problem (P2)

In this subsection, we construct a rank-one solution to problem (P2), as stated in the following proposition.

Proposition 2. Based on the obtained solution $\tilde{\mathbf{W}}^*$, $\tilde{\mathbf{S}}^*$, and $\tilde{\eta}^*$ to problem (P2.1), we can always construct an equivalent solution \mathbf{W}^* , \mathbf{S}^* , and η^* , such that the same objective value in (P2.1) is achieved with $\text{rank}(\mathbf{W}^*) = 1$.

$$\mathbf{W}^* = \frac{\tilde{\mathbf{W}}^* \mathbf{g} \mathbf{g}^H \tilde{\mathbf{W}}^*}{\mathbf{g}^H \tilde{\mathbf{W}}^* \mathbf{g}}, \quad (47a)$$

$$\mathbf{S}^* = \tilde{\mathbf{W}}^* + \tilde{\mathbf{S}}^* - \mathbf{W}^*, \quad (47b)$$

$$\eta^* = \tilde{\eta}^*. \quad (47c)$$

As a result, the constructed solution of \mathbf{W}^* , \mathbf{S}^* , and η^* is a feasible high-quality solution to problem (P2).

Proof. Please refer to Appendix B. □

Remark 2. It is interesting to discuss the relations among the original problem (P2), the relaxed problem (P2.2), and the restricted problem (P2.5). Let Π_1 , Π_2 , and Π_3 denote the feasible regions of \mathbf{W} , \mathbf{S} , and η to (P2), (P2.2), and (P2.5), respectively. It is noting that problem (P2.2) is a relaxed version of (P2) obtained by dropping the rank constraint, and problem (P2.5) is a restricted version of problem (P2.2). Thus, Π_1 is a subset of Π_2 , and Π_3 is a different subset of Π_2 . Therefore, the constructed rank-one solution \mathbf{W}^* , \mathbf{S}^* , and η^* in Proposition 2 are not

necessarily feasible to the corresponding restricted problem (P2.5), though it is ensured to be feasible for (P2). However, it is interesting to find that \mathbf{W}^* , \mathbf{S}^* , and η^* in Proposition 2 are always feasible to problem (P2.5) in our simulations.

Remark 3. By comparing Proposition 1 and Proposition 2, it is interesting to observe that similar construction methods are adopted to construct the desired rank-one solutions, for which the intuitions can be explained as follows. In particular, as the BS has the perfect CSI of the CU in both scenarios, we can always project the general-rank information beamforming matrix $\tilde{\mathbf{W}}^*$ or $\tilde{\mathbf{W}}^*$ into the subspace of the CU's channel (see (30a) or (47a)), which will not affect the SINR at the CU. At the same time, we allocate the remaining power after projection to the sensing/AN beams \mathbf{S}^* or \mathbf{S}^* (see (30b) or (47b)) such that the SINR at all the eavesdroppers would be degraded, thus improving the secure communication performance. As a result, based on such construction methods, we obtain the desired rank-one information beamforming solution for both problems (P1) and (P2).

V. NUMERICAL RESULTS

This section provides numerical results to validate the performance of our proposed joint information and sensing beamforming designs for secure ISAC. In the simulations, the BS is equipped with $N = 8$ antennas. We set the noise powers at the CU and all the eavesdroppers to be identical as -50 dBm, i.e., $\sigma_0^2 = \sigma_k^2 = -50$ dBm, $\forall k \in \mathcal{K}_E$ [7]. We assume that the signal attenuation from the BS to all the targets are identical to be $\varphi = 50$ dB corresponding to an equal distance of 5 meters, and the signal attenuation from the BS to the CU to be $\alpha = 70$ dB corresponding to a distance of 50 meters. Furthermore, the transmit power budget at each antenna of the BS is set to be $Q = \frac{1}{N}$ Watt such that the total transmit power at the BS is 1 Watt or 30 dBm. We choose $M = 500$ angles for $\{\bar{\theta}_m\}$, which are uniformly sampled over $[-\frac{\pi}{2}, \frac{\pi}{2}]$. We also set the width of beampattern angle as $\Delta\theta = 10^\circ$. The normalized spacing between two adjacent antennas is set as $\frac{d}{\lambda} = 0.5$. There are $K = 4$ targets located at angles -15° , 15° , -45° , and 45° , i.e., $\{\theta_k\} = \{\hat{\theta}_k\} = \{-15^\circ, 15^\circ, -45^\circ, 45^\circ\}$, among which the first $K_E = 2$ targets (located at -15° and 15°) are untrusted targets. Furthermore, we consider the LoS channel from the BS to the CU, i.e., $\mathbf{g} = \sqrt{10^{-7}}\mathbf{a}(\theta_0)$. The weight of cross-correlation pattern is set as $\omega_C = 1$. For performance comparison, we consider the separate information and sensing beamforming design as a benchmark scheme as follows.

- **Separate design:** The information and sensing beamformers are separately designed in the following two stages. First, we obtain the information beamforming vector \mathbf{w}_0 or $\mathbf{W} = \mathbf{w}_0\mathbf{w}_0^H$ to minimize the transmit power $\text{Tr}(\mathbf{W})$ while ensuring the secrecy requirements for bounded CSI errors or Gaussian errors (i.e., (21a) and (22a)), respectively. These problems have been well investigated in literature [22], [27]. Denote the obtained information beamforming covariance solution as $\bar{\mathbf{W}}^*$. Next, with the obtained $\bar{\mathbf{W}}^*$, we design the dedicated sensing signal by restricting it in the null space of the CU channel to guarantee the secrecy requirements. Towards this end, we set $\mathbf{S} = \mathbf{Q}_2\bar{\mathbf{S}}_2\mathbf{Q}_2^H$, where $\mathbf{Q}_2 = \mathbf{I} - \mathbf{g}\mathbf{g}^H/\|\mathbf{g}\|^2$. Then, we optimize the sensing beampattern subject to a power constraint as

$$\begin{aligned} \min_{\bar{\mathbf{S}}_2 \succeq \mathbf{0}, \eta} \quad & \frac{1}{M} \sum_{m=1}^M \left| \eta \hat{P}(\bar{\theta}_m) - \mathbf{a}^H(\bar{\theta}_m)(\bar{\mathbf{W}}^* + \mathbf{Q}_2\bar{\mathbf{S}}_2\mathbf{Q}_2^H)\mathbf{a}(\bar{\theta}_m) \right|^2 \\ & + \frac{2\omega_C}{K^2 - K} \sum_{p=1}^K \sum_{q=p+1}^K \left| \mathbf{a}^H(\hat{\theta}_p)(\bar{\mathbf{W}}^* + \mathbf{Q}_2\bar{\mathbf{S}}_2\mathbf{Q}_2^H)\mathbf{a}(\hat{\theta}_q) \right|^2 \\ \text{s.t.} \quad & \text{Tr}(\mathbf{E}_i\mathbf{Q}_2\bar{\mathbf{S}}_2\mathbf{Q}_2^H + \mathbf{E}_i\bar{\mathbf{W}}^*) = Q, \forall i \in \{1, \dots, N\}. \end{aligned} \quad (48)$$

Problem (48) is a convex optimization problem that can be solved via CVX, for which the optimal solution is obtained by $\bar{\mathbf{S}}_2^*$. Accordingly, we have the sensing beamformers as $\bar{\mathbf{S}}^* = \mathbf{Q}_2\bar{\mathbf{S}}_2^*\mathbf{Q}_2^H$.

In Section V-A, we first evaluate the performance of our proposed design in the special case with perfect CSI, which corresponds to (P1) with $\mathbf{e}_k = \mathbf{0}$ or (P2) with $\mathbf{C}_k = \mathbf{0}$, $\forall k \in \mathcal{K}_E$, and $\rho = 0$ (see Remark 1), as compared to the separate design benchmark. In Section V-B and Section V-C, we consider the two scenarios with bounded and Gaussian CSI errors of eavesdroppers, respectively.

A. Special Case with Perfect CSI

In this subsection, we consider the special case with perfect CSI. In this case, we assume LoS channels from the BS to all the potential eavesdroppers with $\mathbf{h}_k = \sqrt{10^{-3}}\mathbf{a}(\theta_k)$, $\forall k \in \mathcal{K}_E$.

First, Fig. 2 shows the achieved transmit beampatterns by the proposed design (i.e., the joint information and sensing beampattern), in which the secrecy rate threshold is set as $R_0 = 4$ bps/Hz, and the CU is located at $\theta_0 = 0^\circ$. To reveal more insights and for comparison, we also show the transmit information beampattern part (i.e., $\mathbf{a}^H(\theta)\mathbf{W}\mathbf{a}(\theta)$ achieved by the information signals \mathbf{W} only) and the dedicated sensing signal beampattern part (i.e., $\mathbf{a}^H(\theta)\mathbf{S}\mathbf{a}(\theta)$ achieved

by the sensing signals \mathbf{S} only) under our proposed design, as well as the optimal sensing-only beampattern $\mathbf{a}^H(\theta)\mathbf{R}_{\text{sen}}\mathbf{a}(\theta)$, where \mathbf{R}_{sen} is obtained by solving the sensing beampattern optimization problem (e.g., (P1) with $R_0 = 0$ bps/Hz). It is observed that the information signal beampatterns are designed towards the CU, while the sensing signal beampatterns are designed towards both untrusted and trusted targets, thus maximizing the sensing performance while ensuring the CU's secure communication requirements. It is also observed that there is a significant discrepancy between the achieved joint beampattern and the desired beampattern at the angle of CU (0°), as the information signal beams need to be steered towards this direction to satisfy the secure communication requirement. Furthermore, for the proximate angles of the eavesdropping targets, the information signal beams are suppressed substantially to reduce the potential of information leakage, while the energies of sensing signal beams are focused on these angles to ensure the sensing requirements and degrade the quality of the eavesdropping channels.

Fig. 3 shows the sensing beampattern error $D(\mathbf{W}, \mathbf{S}, \eta)$ versus the secrecy rate threshold R_0 with $\theta_0 = 3^\circ$. It is observed that in the whole regime of R_0 , the proposed optimal design achieves lower sensing beampattern errors than that of the separate design benchmark scheme. The performance gap is around 20% of the sensing beampattern error achieved by the sensing-only benchmark. When R_0 becomes sufficiently low, the optimal design approaches the error lower bound obtained by the sensing-only benchmark, but the separate design performs worse than the optimal design. This is because for the separate design, the sensing beam is designed within the null space of the CU channel, thus limiting the available design DoF for sensing and degrading its performance.

Fig. 4 shows the sensing beampattern error $D(\mathbf{W}, \mathbf{S}, \eta)$ versus the CU angle θ_0 , with $R_0 = 4$ bps/Hz. Notice that the secrecy rate constraint $R_0 = 4$ bps/Hz cannot be satisfied when $\theta_0 \in (-20^\circ, -10^\circ) \cup (10^\circ, 20^\circ)$, as the CU is in the neighborhood of the eavesdropping targets such that no secure information transmission is feasible. As a result, there is no sensing beampattern error shown in these regions. First, it is observed that the separate design performs inferior to our proposed optimal design in term of sensing beampattern error. This is consistent with the observation in Fig. 3. When the CU is located close to a trusted target (i.e., $\theta_0 = -45^\circ$ and 45°), the sensing beampattern error is observed to be low, as the information signals play the dual role of communicating with the CU and sensing the trusted target concurrently.

Furthermore, besides showing the behaviors of the transmit beampatterns, we also show the

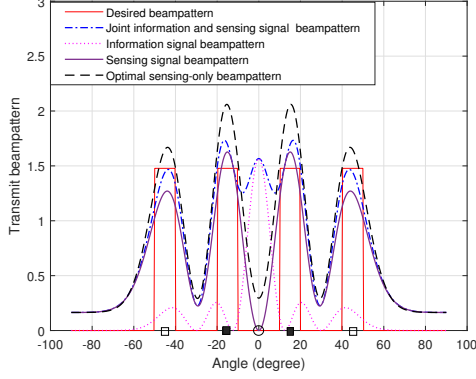


Fig. 2: The transmit beampatterns in the special case of perfect CSI, where $R_0 = 4$ bps/Hz. The circle indicates the CU angle, the solid rectangles indicate the untrusted target angles, and the hollow rectangles indicate the trusted ones.

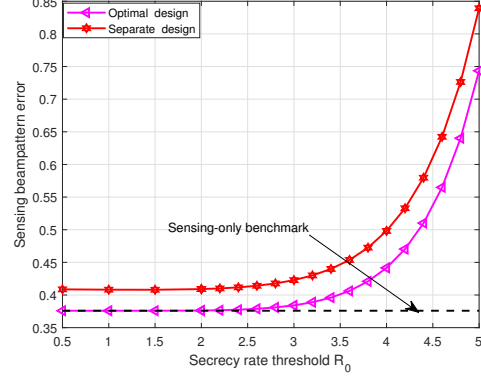


Fig. 3: The sensing beampattern error $D(\mathbf{W}, \mathbf{S}, \eta)$ versus the secrecy rate threshold R_0 in the special case of perfect CSI.

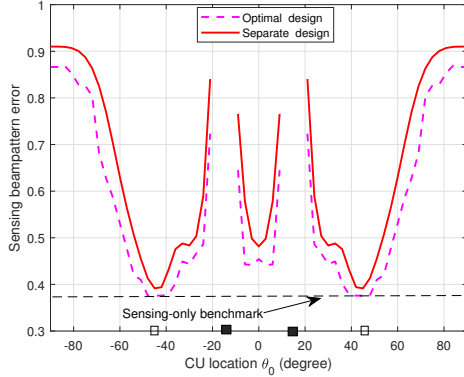


Fig. 4: The sensing beampattern error $D(\mathbf{W}, \mathbf{S}, \eta)$ versus the CU angle θ_0 in the special case of perfect CSI. The solid rectangles indicate untrusted target angles, and the hollow rectangles indicate trusted ones.

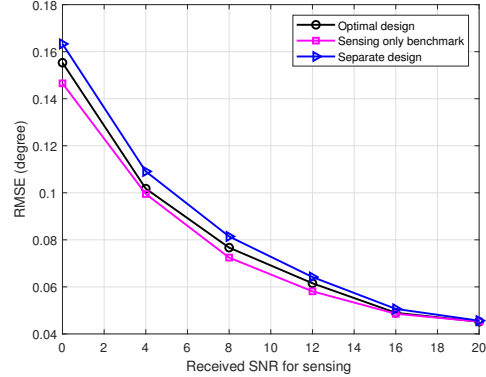


Fig. 5: RMSE versus the received SNR for sensing with perfect CSI.

actual angle estimation performance of multiple targets at the BS sensing receiver to validate the efficiency of our proposed joint transmit beamforming design. In the simulation, we consider the sequence with a number of $L = 256$ symbols for multi-target estimation, in which the transmit signal $\mathbf{x}(n) = \mathbf{w}_0 s_0(n) + \mathbf{S}^{1/2} \mathbf{u}(n)$ in each symbol n is generated based on $\mathbf{u}(n) \sim \mathcal{CN}(\mathbf{0}, \mathbf{I})$ and $s_0(n) \sim \mathcal{CN}(0, 1)$, $n \in \{1, \dots, L\}$. Also, we adopt the sample correlation matrix $\mathbf{R}_{xx} = \frac{1}{L} \sum_{n=1}^L \mathbf{x}(n) \mathbf{x}^H(n)$ to approximate the transmit covariance matrix $\mathbf{W} + \mathbf{S}$. It was shown in [19]

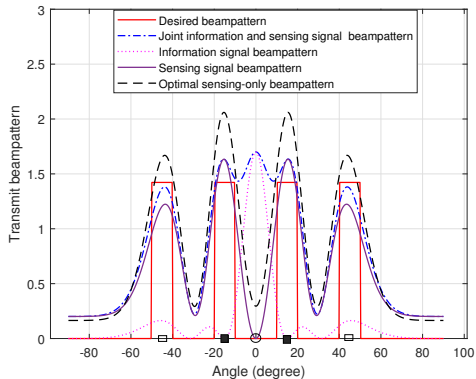


Fig. 6: Transmit beampattern with bounded CSI errors, $R_0 = 4$ bps/Hz, $\mu = 0.3$. The circle indicates the direction of the CU and the rectangles indicate directions of targets with solid rectangles for the untrusted ones and hollow rectangles for the trusted ones.

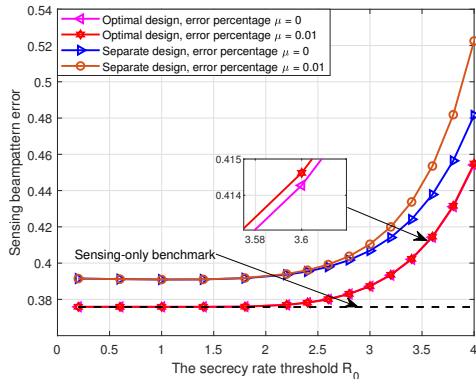


Fig. 7: The sensing beampattern error $D(\mathbf{W}, \mathbf{S}, \eta)$ versus the worst-case secrecy rate threshold R_0 with bounded CSI errors of eavesdroppers.

that their difference is quite small when the sample length $L = 256$. Accordingly, the angles $\{\theta_k\}$ are estimated based on the received signals in (4) via the Capon technique [20]. In particular, the Capon spatial spectrum is obtained as

$$\frac{|\mathbf{a}^H(\theta)\mathbf{R}_{yy}^{-1}\mathbf{R}_{yx}\mathbf{a}(\theta)|}{(\mathbf{a}^H(\theta)\mathbf{R}_{yy}^{-1}\mathbf{a}(\theta))(\mathbf{a}^T(\theta)\mathbf{R}_{xx}\mathbf{a}^c(\theta))}, \quad (49)$$

where $\mathbf{R}_{yy} = \frac{1}{L} \sum_{n=1}^L \mathbf{y}(n)\mathbf{y}^H(n)$, $\mathbf{R}_{xx} = \frac{1}{L} \sum_{n=1}^L \mathbf{x}(n)\mathbf{x}^H(n)$, and $\mathbf{R}_{yx} = \frac{1}{L} \sum_{n=1}^L \mathbf{y}(n)\mathbf{x}^H(n)$. In the implementation of the Capon technique, we uniformly divide $[-\frac{\pi}{2}, \frac{\pi}{2}]$ into 1000 grids to generate the Capon spatial spectrum, and accordingly find the estimated angles as the K ones with peak spectrum values.

Fig. 5 shows the angle estimation root mean squared error (RMSE) by the Capon technique versus the received SNR for sensing at the BS, which is obtained by averaging over 1000 random realizations. Here, the RMSE is defined as $\text{RMSE} = \sqrt{\frac{1}{K} \sum_{k=1}^K (\tilde{\theta}_k - \theta_k)^2}$, where $\{\tilde{\theta}_k\}$ denote the estimate of $\{\theta_k\}$. It is observed that the sensing-only benchmark achieves the best sensing performance. Furthermore, the proposed optimal design is observed to lead to a lower RMSE than the separate design. This shows that our design for minimizing the sensing beampattern error is efficient in enhancing the multi-target angle estimation accuracy, since minimizing the cross-correlation pattern in (19) ensures the resolution of different angles and minimizing the beampattern matching MSE in (18) ensures the energy towards directions of angles.

B. Scenario with Bounded CSI Errors

Next, we consider the scenario with bounded CSI errors of eavesdroppers, in which the estimated channels of each eavesdropping target are set as $\hat{\mathbf{h}}_k = \sqrt{10^{-3}}\mathbf{a}(\theta_k)$, $\forall k \in \mathcal{K}_E$, and the corresponding CSI error bound is set as $\varepsilon_k = \mu|\hat{\mathbf{h}}_k|$, $\forall k \in \mathcal{K}_E$, where μ denotes the error percentage. The CU is located at angle $\theta_0 = 0^\circ$.

Fig. 6 shows the achieved transmit beampattern, where $R_0 = 4$ bps/Hz and $\mu = 0.3$. By comparing it versus the transmit beampattern with perfect CSI in Fig. 2, it is observed that the information beampattern at the CU angle of 0° becomes narrower for the purpose of strengthening the confidential information transmission to combat the potential information leakage caused by the uncertain eavesdropping channels. Furthermore, the information transmit beampattern is observed to be further suppressed at proximate angles of these untrusted targets (-15° and 15°) compared to the case of perfect CSI. As such, the transmit beampatterns around these untrusted targets are observed to be provided by the sensing signal beampatterns only, which also help further prevent potential eavesdropping.

Next, we consider the performance comparison of separate design benchmark and the optimal design in the bounded CSI errors case. Fig. 7 shows the sensing beampattern error $D(\mathcal{S}, \mathbf{W}, \eta)$ versus the secrecy rate threshold R_0 , in which two different error percentages (i.e., $\mu = 0.01$ and 0) are considered. It is observed that the performance gap between the separate design benchmark and the optimal (robust) design becomes more significant in the bounded CSI errors case ($\mu = 0.01$) than that of the case of perfect CSI, which indicates that the separate design is actually not robust against errors. This is due to the fact in the separate design, when deriving the information beamforming vector, we do not consider the AN role of sensing signals in degrading the quality of eavesdropping channels. Thus, this leads to inactive secure communication requirement constraints and more energy is allocated to the information beamformers than that needed in the optimal design. The redundant power allocation for information beamforming in the scenario with bounded CSI errors deteriorates the sensing performance. It is also observed that higher eavesdropping channel uncertainty (or a larger value of μ) leads to more significant sensing beampattern errors, as more transmit power is allocated to ensure secure communication, thus causing more severe beampattern distortion.

Then, we evaluate the angle estimation performance of the separate design and the optimal design via the Capon technique. Fig. 8 shows the estimation RMSE versus the received SNR for

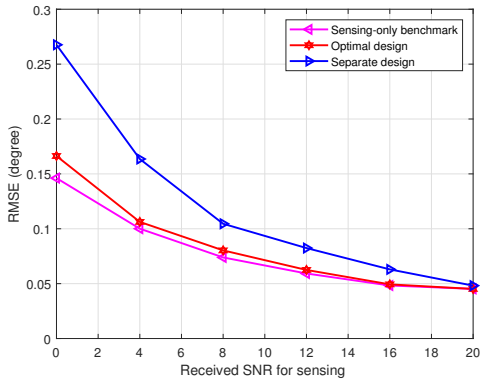


Fig. 8: RMSE versus received SNR for sensing with bounded CSI errors.

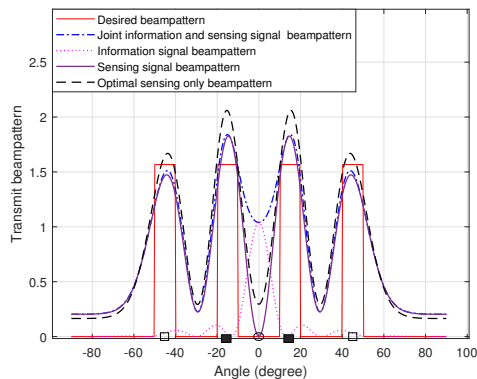


Fig. 9: Transmit beampattern with Gaussian CSI errors, $R_0 = 2.5$ bps/Hz, $\rho = 0.1$. The circle indicates the direction of the CU and the rectangles indicate directions of targets with solid rectangles for the untrusted ones and hollow rectangles for the trusted ones.

sensing, where the error percentage μ is set as 0.02. For comparison, we also show the sensing performance achieved by the sensing-only benchmark. It is observed that the sensing performance of the optimal design is significantly better than the separate design and performs close to the sensing-only benchmark, especially when the SNR becomes large. This shows the robustness of our proposed designs to the bounded CSI errors and is consistent with the observation in Fig. 7.

C. Scenario with Gaussian CSI Errors

Furthermore, we consider the scenario with Gaussian CSI errors of eavesdroppers. We consider the Rician fading channels from the BS to all eavesdroppers, i.e., $\mathbf{h}_k = \sqrt{\frac{K_R}{K_R+1}} \mathbf{h}_k^{\text{LoS}} + \sqrt{\frac{1}{K_R+1}} \mathbf{h}_k^{\text{NLoS}}$, $\forall k \in \mathcal{K}_E$, where $K_R = 10$ is the Rician factor, $\hat{\mathbf{h}}_k = \sqrt{\frac{K_R}{K_R+1}} \mathbf{h}_k^{\text{LoS}} = \sqrt{\frac{K_R}{K_R+1}} \sqrt{10^{-3}} \mathbf{a}(\theta_k)$, and $\mathbf{h}_k^{\text{NLoS}} \sim \mathcal{CN}(\mathbf{0}, 10^{-3} \mathbf{I})$, $\forall k \in \mathcal{K}_E$. We set the estimated channel as $\hat{\mathbf{h}}_k$ and $\mathbf{C}_k = \frac{1}{K_R+1} 10^{-3} \mathbf{I}$ for each eavesdropping target k . In the case of Gaussian CSI errors, the separate design benchmark is highly sub-optimal, which may become infeasible for problem (P2) when the secrecy rate and outage probability requirements become stringent. Therefore, we do not consider the separate design in this subsection, but focus on examining the impact of the secrecy rate threshold R_0 and the outage threshold ρ .

Fig. 9 shows the achieved transmit beampattern with $R_0 = 2.5$ bps/Hz and the outage threshold $\rho = 0.1$. It is observed that the information signal beam is designed towards the CU angle to

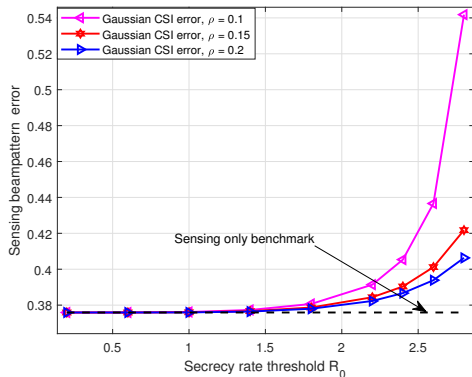


Fig. 10: The sensing beampattern error $D(\mathbf{W}, \mathcal{S}, \eta)$ versus the secrecy rate threshold R_0 .

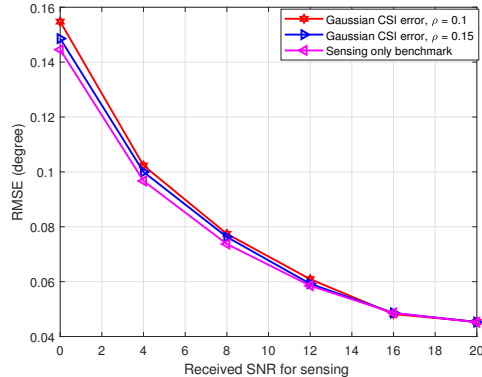


Fig. 11: RMSE versus received SNR for sensing with Gaussian CSI errors.

ensure secure communication with Gaussian CSI errors of eavesdroppers, which is similar to the observation in Fig. 2 with perfect CSI and that in Fig. 6 with the bounded CSI errors.

Fig. 10 shows the sensing beampattern error $D(\mathbf{W}, \mathcal{S}, \eta)$ versus the secrecy rate threshold R_0 , in which ρ is set as 0.1, 0.15, and 0.2. It is observed that the sensing beampattern error increases when ρ becomes small. This is due to the fact that the secrecy outage constraint becomes stricter in this case, and more transmit power should be allocated to information signals towards the CU direction.

Next, Fig. 11 shows the estimation RMSE versus received SNR for sensing, in which ρ is set as 0.1 and 0.15. It is observed that a lower outage threshold of ρ leads to a higher estimation RMSE. This is because stricter secrecy outage requirement leads to a higher sensing beampattern error (see Fig. 10) with more severe beampattern distortion and higher cross-correlation patterns, thus resulting in worse sensing performance. Our proposed optimal design is observed to achieve RMSE close to the sensing-only benchmark. This shows the robustness of our proposed design against Gaussian CSI errors.

VI. CONCLUSION

This paper studied the robust transmit beamforming problem for a secure ISAC system that consists of a BS, a single CU, and multiple sensing targets. We considered the case of imperfect CSI of eavesdroppers subject to bounded errors and Gaussian errors, and formulated the worst-case secrecy rate and the secrecy outage constrained beampattern optimization problems, respectively. Then, we optimally solved the worst-case secrecy rate constrained beampattern

matching problem by using the technique of S-procedure, SDR, and 1D search, and rigorously proved the tightness of the SDR. Next, to solve the secrecy outage constrained beam pattern matching problem, we adopted the safe approximation based on the BTI to obtain a restricted problem, then solved the restricted problem using the technique of SDR and 1D search, and finally constructed a high-quality solution to the original problem. Finally, we provided numerical results to evaluate the transmit beam pattern and the sensing performance, showing the non-trivial tradeoff between secure communication and sensing. It was shown that our proposed robust design adjusts the information and sensing beams to balance the tradeoffs among communicating with CU, sensing targets, and confusing eavesdroppers, and achieve desirable sensing transmit beam patterns while ensuring the CU's secrecy requirements.

APPENDIX A

PROOF OF PROPOSITION 1

First, it is observed from (30b) that $\mathbf{S}^* + \mathbf{W}^* = \tilde{\mathbf{W}}^* + \tilde{\mathbf{S}}^*$. As a result, \mathbf{W}^* , \mathbf{S}^* , and η^* achieve the same objective value for problem (P1.3) as that achieved by $\tilde{\mathbf{W}}^*$, $\tilde{\mathbf{S}}^*$, and $\tilde{\eta}^*$. Note that \mathbf{W}^* , \mathbf{S}^* also satisfy the constraints in (21b) and (21c).

Next, since $\tilde{\mathbf{W}}^* \succeq \mathbf{0}$, we have $\tilde{\mathbf{W}}^* = \mathbf{F}\mathbf{F}^H$. Based on this, for any $\mathbf{v} \in \mathbb{C}^{N \times 1}$, it follows that

$$\begin{aligned} \mathbf{v}^H (\tilde{\mathbf{W}}^* - \mathbf{W}^*) \mathbf{v} &= \mathbf{v}^H \tilde{\mathbf{W}}^* \mathbf{v} - \mathbf{v}^H \frac{\tilde{\mathbf{W}}^* \mathbf{g} \mathbf{g}^H \tilde{\mathbf{W}}^*}{\mathbf{g}^H \tilde{\mathbf{W}}^* \mathbf{g}} \mathbf{v} \\ &= \frac{1}{\mathbf{g}^H \tilde{\mathbf{W}}^* \mathbf{g}} (\mathbf{v}^H \tilde{\mathbf{W}}^* \mathbf{v} \mathbf{g}^H \tilde{\mathbf{W}}^* \mathbf{g} - \mathbf{v}^H \tilde{\mathbf{W}}^* \mathbf{g} \mathbf{g}^H \tilde{\mathbf{W}}^* \mathbf{v}) \\ &= \frac{1}{\mathbf{g}^H \tilde{\mathbf{W}}^* \mathbf{g}} (\|\mathbf{a}\|^2 \|\mathbf{b}\|^2 - |\mathbf{a}^H \mathbf{b}|^2) \stackrel{(a)}{\geq} 0, \end{aligned} \quad (50)$$

where $\mathbf{a} = \mathbf{F}^H \mathbf{v} \in \mathbb{C}^{N \times 1}$, $\mathbf{b} = \mathbf{F}^H \mathbf{g} \in \mathbb{C}^{N \times 1}$, and inequality (a) holds because of the Cauchy-Schwartz inequality. Accordingly, we have $\tilde{\mathbf{W}}^* - \mathbf{W}^* \succeq \mathbf{0}$. By using this together with (30b), we have $\mathbf{S}^* \succeq \tilde{\mathbf{S}}^* \succeq \mathbf{0}$.

Furthermore, we prove that \mathbf{W}^* , \mathbf{S}^* , γ^* , η^* , and $\{\lambda_k^*\}$ satisfy the constraints in (24a) and (27). On the one hand, it is clear from (30a) and (30b) that $\mathbf{g}^H \tilde{\mathbf{W}}^* \mathbf{g} = \mathbf{g}^H \mathbf{W}^* \mathbf{g}$ and $\mathbf{g}^H \tilde{\mathbf{S}}^* \mathbf{g} = \mathbf{g}^H \mathbf{S}^* \mathbf{g}$, and therefore constraint (24a) holds. On the other hand, as $\tilde{\mathbf{W}}^*$, $\tilde{\mathbf{S}}^*$, $\tilde{\gamma}^*$, $\tilde{\eta}^*$, and $\{\tilde{\lambda}_k^*\}$ satisfy the constraint in (27), we have

$$\begin{bmatrix} \tilde{\lambda}_k^* \mathbf{I} - (\tilde{\mathbf{W}}^* - \varphi(\tilde{\gamma}^*) \tilde{\mathbf{S}}^*) & -(\tilde{\mathbf{W}}^* - \varphi(\tilde{\gamma}^*) \tilde{\mathbf{S}}^*) \hat{\mathbf{h}}_k \\ -\hat{\mathbf{h}}_k^H (\tilde{\mathbf{W}}^* - \varphi(\tilde{\gamma}^*) \tilde{\mathbf{S}}^*) & -\tilde{\lambda}_k^* \varepsilon_k^2 - \hat{\mathbf{h}}_k^H (\tilde{\mathbf{W}}^* - \varphi(\tilde{\gamma}^*) \tilde{\mathbf{S}}^*) \hat{\mathbf{h}}_k + \varphi(\tilde{\gamma}^*) \sigma_k^2 \end{bmatrix} \succeq \mathbf{0}, \quad \forall k \in \mathcal{K}_E.$$

It follows that

$$\begin{aligned}
& \begin{bmatrix} \lambda_k^* \mathbf{I} - (\mathbf{W}^* - \varphi(\gamma^*) \mathbf{S}^*) & -(\mathbf{W}^* - \varphi(\gamma^*) \mathbf{S}^*) \hat{\mathbf{h}}_k \\ -\hat{\mathbf{h}}_k^H (\mathbf{W}^* - \varphi(\gamma^*) \mathbf{S}^*) & -\lambda_k^* \varepsilon_k^2 - \hat{\mathbf{h}}_k^H (\mathbf{W}^* - \varphi(\gamma^*) \mathbf{S}^*) \hat{\mathbf{h}}_k + \varphi(\gamma^*) \sigma_k^2 \end{bmatrix} \\
- & \begin{bmatrix} \tilde{\lambda}_k^* \mathbf{I} - (\tilde{\mathbf{W}}^* - \varphi(\tilde{\gamma}^*) \tilde{\mathbf{S}}^*) & -(\tilde{\mathbf{W}}^* - \varphi(\tilde{\gamma}^*) \tilde{\mathbf{S}}^*) \hat{\mathbf{h}}_k \\ -\hat{\mathbf{h}}_k^H (\tilde{\mathbf{W}}^* - \varphi(\tilde{\gamma}^*) \tilde{\mathbf{S}}^*) & -\tilde{\lambda}_k^* \varepsilon_k^2 - \hat{\mathbf{h}}_k^H (\tilde{\mathbf{W}}^* - \varphi(\tilde{\gamma}^*) \tilde{\mathbf{S}}^*) \hat{\mathbf{h}}_k + \varphi(\tilde{\gamma}^*) \sigma_k^2 \end{bmatrix} \\
= & \begin{bmatrix} \Delta \mathbf{W} - \varphi(\gamma^*) \Delta \mathbf{S} & (\Delta \mathbf{W} - \varphi(\gamma^*) \Delta \mathbf{S}) \hat{\mathbf{h}}_k \\ \hat{\mathbf{h}}_k^H (\Delta \mathbf{W} - \varphi(\gamma^*) \Delta \mathbf{S}) & \hat{\mathbf{h}}_k^H (\Delta \mathbf{W} - \varphi(\gamma^*) \Delta \mathbf{S}) \hat{\mathbf{h}}_k \end{bmatrix}, \forall k \in \mathcal{K}_E, \quad (51)
\end{aligned}$$

where $\Delta \mathbf{W} = \tilde{\mathbf{W}}^* - \mathbf{W}^* \succeq \mathbf{0}$, $\Delta \mathbf{S} = \tilde{\mathbf{S}}^* - \mathbf{S}^* \preceq \mathbf{0}$, and thus $\Delta \mathbf{W} - \varphi(\gamma^*) \Delta \mathbf{S} \succeq \mathbf{0}$. Therefore, we only need to prove that the right-hand-side (RHS) of (51) is positive semi-definite to satisfy (27). Towards this end, we introduce the following theorem about positive semi-definite block matrices.

Theorem 1. [28] Let $\mathbf{H} = \begin{bmatrix} \mathbf{A} & \mathbf{B} \\ \mathbf{B}^H & \mathbf{C} \end{bmatrix} \in \mathbb{S}^{L+T}$, with $\mathbf{A} \in \mathbb{S}^L$ and $\mathbf{C} \in \mathbb{S}^T$. The following two statements are equivalent:

(a) \mathbf{H} is positive semi-definite.

(b) \mathbf{A} and \mathbf{C} are positive semi-definite, and there is a contraction $\mathbf{X} \in \mathbb{C}^{L \times T}$ such that $\mathbf{B} = \mathbf{A}^{1/2} \mathbf{X} \mathbf{C}^{1/2}$.

A given matrix is a contraction if its largest singular value is less than or equal to 1. Recall that $\Delta \mathbf{W} - \varphi(\gamma^*) \Delta \mathbf{S} \succeq \mathbf{0}$, we have $\hat{\mathbf{h}}_k^H (\Delta \mathbf{W} - \varphi(\gamma^*) \Delta \mathbf{S}) \hat{\mathbf{h}}_k \geq 0$. Here, notice that $\left(\hat{\mathbf{h}}_k^H (\Delta \mathbf{W} - \varphi(\gamma^*) \Delta \mathbf{S}) \hat{\mathbf{h}}_k \right)^{1/2} = \|(\Delta \mathbf{W} - \varphi(\gamma^*) \Delta \mathbf{S})^{1/2} \hat{\mathbf{h}}_k\|$. Then, we select

$$\mathbf{a} = \frac{1}{\|(\Delta \mathbf{W} - \varphi(\gamma^*) \Delta \mathbf{S})^{1/2} \hat{\mathbf{h}}_k\|} \cdot (\Delta \mathbf{W} - \varphi(\gamma^*) \Delta \mathbf{S})^{1/2} \hat{\mathbf{h}}_k. \quad (52)$$

Due to $\|\mathbf{a}\| = 1$, \mathbf{a} is a contraction. Thus, we have

$$(\Delta \mathbf{W} - \varphi(\gamma^*) \Delta \mathbf{S})^{1/2} \mathbf{a} \|(\Delta \mathbf{W} - \varphi(\gamma^*) \Delta \mathbf{S})^{1/2} \hat{\mathbf{h}}_k\| = (\Delta \mathbf{W} - \varphi(\gamma^*) \Delta \mathbf{S}) \hat{\mathbf{h}}_k. \quad (53)$$

By combining $\Delta \mathbf{W} - \varphi(\gamma^*) \Delta \mathbf{S} \succeq \mathbf{0}$ and (53), we prove that the RHS of (51) is positive semi-definite. As a result, constraint (27) is satisfied.

By combining the results above, it is proved that \mathbf{W}^* , \mathbf{S}^* , γ^* , η^* , and $\{\lambda_k^*\}$ are optimal for problem (P1.3). Notice that $\text{rank}(\mathbf{W}^*) = 1$. This thus completes the proof.

APPENDIX B

PROOF OF PROPOSITION 2

Based on the similar proof techniques as in Appendix A, we have

$$\mathbf{S}^* \succeq \tilde{\mathbf{S}}^* \succeq \mathbf{0}, \quad (54)$$

$$\tilde{\mathbf{W}}^* \succeq \mathbf{W}^* \succeq \mathbf{0}, \quad (55)$$

$$\tilde{\mathbf{W}}^* + \tilde{\mathbf{S}}^* = \mathbf{W}^* + \mathbf{S}^*. \quad (56)$$

It follows from (56) that \mathbf{W}^* , \mathbf{S}^* , and η^* achieve the same objective value for $D(\mathbf{W}, \mathbf{S}, \eta)$ as that achieved by $\tilde{\mathbf{W}}^*$, $\tilde{\mathbf{S}}^*$, and $\tilde{\eta}^*$. Therefore, we need to verify that the constructed solution \mathbf{W}^* , \mathbf{S}^* , and η^* satisfy (31), (22b), and (22c). Based on (56), $\mathbf{g}^H \tilde{\mathbf{W}}^* \mathbf{g} = \mathbf{g}^H \mathbf{W}^* \mathbf{g}$, and $\mathbf{g}^H \tilde{\mathbf{S}}^* \mathbf{g} = \mathbf{g}^H \mathbf{S}^* \mathbf{g}$, (22b) and (22c) are satisfied. Then, we focus on proving that (31) is satisfied.

Based on (54) and (55), we have

$$\frac{\mathbf{h}_k^H \mathbf{W}^* \mathbf{h}_k}{\mathbf{h}_k^H \mathbf{S}^* \mathbf{h}_k + \sigma_k^2} \leq \frac{\mathbf{h}_k^H \tilde{\mathbf{W}}^* \mathbf{h}_k}{\mathbf{h}_k^H \tilde{\mathbf{S}}^* \mathbf{h}_k + \sigma_k^2}, \forall \mathbf{h}_k \in \mathbb{C}^{N \times 1}. \quad (57)$$

As a result,

$$\begin{aligned} & \Pr\left(\log_2(1 + \gamma) - \max_{k \in \mathcal{K}_E} \log_2\left(1 + \frac{\mathbf{h}_k^H \mathbf{W}^* \mathbf{h}_k}{\mathbf{h}_k^H \mathbf{S}^* \mathbf{h}_k + \sigma_k^2}\right) \geq R_0\right) \\ & \geq \Pr\left(\log_2(1 + \gamma) - \max_{k \in \mathcal{K}_E} \log_2\left(1 + \frac{\mathbf{h}_k^H \tilde{\mathbf{W}}^* \mathbf{h}_k}{\mathbf{h}_k^H \tilde{\mathbf{S}}^* \mathbf{h}_k + \sigma_k^2}\right) \geq R_0\right) \geq 1 - \rho. \end{aligned} \quad (58)$$

This completes the proof.

REFERENCES

- [1] Z. Ren, L. Qiu, and J. Xu, "Optimal transmit beamforming for secrecy integrated sensing and communication," to appear in *IEEE Int. Conf. Commun. (ICC)*, May 2022.
- [2] F. Liu, C. Masouros, A. P. Petropulu, H. Griffiths, and L. Hanzo, "Joint radar and communication design: Applications, state-of-the-art, and the road ahead," *IEEE Trans. Commun.*, vol. 68, no. 6, pp. 3834–3862, Feb. 2020.
- [3] M. L. Rahman, J. A. Zhang, X. Huang, Y. J. Guo, and R. W. Heath, "Framework for a perceptive mobile network using joint communication and radar sensing," *IEEE Trans. Aerosp. Electron. Syst.*, vol. 56, no. 3, pp. 1926–1941, Jun. 2020.
- [4] F. Liu, Y. Cui, C. Masouros, J. Xu, T. X. Han, Y. C. Eldar, and S. Buzzi, "Integrated sensing and communications: Towards dual-functional wireless networks for 6G and beyond," *IEEE J. Sel. Areas Commun.*, vol. 40, no. 6, pp. 1728–1767, Jun. 2022.
- [5] Q. Wu, J. Xu, Y. Zeng, D. W. K. Ng, N. Al-Dhahir, R. Schober, and A. L. Swindlehurst, "A comprehensive overview on 5G-and-beyond networks with UAVs: From communications to sensing and intelligence," *IEEE J. Sel. Areas Commun.*, vol. 39, no. 10, pp. 2912–2945, Oct. 2021.
- [6] X. Liu, T. Huang, N. Shlezinger, Y. Liu, J. Zhou, and Y. C. Eldar, "Joint transmit beamforming for multiuser MIMO communications and MIMO radar," *IEEE Trans. Signal Process.*, vol. 68, pp. 3929–3944, Jun. 2020.

- [7] H. Hua, J. Xu, and T. X. Han, "Optimal transmit beamforming for integrated sensing and communication," *arXiv preprint arXiv:2104.11871*, 2021.
- [8] F. Liu, L. Zhou, C. Masouros, A. Li, W. Luo, and A. Petropulu, "Toward dual-functional radar-communication systems: Optimal waveform design," *IEEE Trans. Signal Process.*, vol. 66, no. 16, pp. 4264–4279, Aug. 2018.
- [9] C. Shi, F. Wang, S. Salous, and J. Zhou, "Joint subcarrier assignment and power allocation strategy for integrated radar and communications system based on power minimization," *IEEE Sens. J.*, vol. 19, no. 23, pp. 11 167–11 179, Dec. 2019.
- [10] A. Deligiannis, A. Daniyan, S. Lambotharan, and J. A. Chambers, "Secrecy rate optimizations for MIMO communication radar," *IEEE Trans. Aerosp. Electron. Syst.*, vol. 54, no. 5, pp. 2481–2492, Oct. 2018.
- [11] N. Su, F. Liu, and C. Masouros, "Secure radar-communication systems with malicious targets: Integrating radar, communications, and jamming functionalities," *IEEE Trans. Wireless Commun.*, vol. 20, no. 1, pp. 83–95, Jan. 2021.
- [12] Z. Wei, F. Liu, C. Masouros, N. Su, and A. P. Petropulu, "Toward multi-functional 6G wireless networks: Integrating sensing, communication, and security," *IEEE Commun. Mag.*, vol. 60, no. 4, pp. 65–71, Apr. 2022.
- [13] A. D. Wyner, "The wire-tap channel," *Bell Syst. Tech. J.*, vol. 54, no. 8, pp. 1355–1387, Oct. 1975.
- [14] P. K. Gopala, L. Lai, and H. El Gamal, "On the secrecy capacity of fading channels," *IEEE Trans. Inf. Theory*, vol. 54, no. 10, pp. 4687–4698, Sep. 2008.
- [15] X. Chen, D. W. K. Ng, W. H. Gerstacker, and H.-H. Chen, "A survey on multiple-antenna techniques for physical layer security," *IEEE Commun. Surveys Tuts.*, vol. 19, no. 2, pp. 1027–1053, 2nd Quart. 2017.
- [16] S. Goel and R. Negi, "Guaranteeing secrecy using artificial noise," *IEEE Trans. Wireless Commun.*, vol. 7, no. 6, pp. 2180–2189, Jun. 2008.
- [17] Y. Wu, A. Khisti, C. Xiao, G. Caire, K.-K. Wong, and X. Gao, "A survey of physical layer security techniques for 5G wireless networks and challenges ahead," *IEEE J. Sel. Areas Commun.*, vol. 36, no. 4, pp. 679–695, Apr. 2018.
- [18] D. Wang, B. Bai, W. Zhao, and Z. Han, "A survey of optimization approaches for wireless physical layer security," *IEEE Commun. Surveys Tuts.*, vol. 21, no. 2, pp. 1878–1911, 2nd Quart. 2019.
- [19] P. Stoica, J. Li, and Y. Xie, "On probing signal design for MIMO radar," *IEEE Trans. Signal Process.*, vol. 55, no. 8, pp. 4151–4161, Aug. 2007.
- [20] L. Xu, J. Li, and P. Stoica, "Target detection and parameter estimation for MIMO radar systems," *IEEE Trans. Aerosp. Electron. Syst.*, vol. 44, no. 3, pp. 927–939, Jul. 2008.
- [21] J. Li and P. Stoica, "MIMO radar with colocated antennas," *IEEE Signal Processing Mag.*, vol. 24, no. 5, pp. 106–114, Sep. 2007.
- [22] J. Huang and A. L. Swindlehurst, "Robust secure transmission in MISO channels based on worst-case optimization," *IEEE Trans. Signal Process.*, vol. 60, no. 4, pp. 1696–1707, Dec. 2011.
- [23] Q. Li, W.-K. Ma, and A. M.-C. So, "A safe approximation approach to secrecy outage design for MIMO wiretap channels," *IEEE Signal Process. Lett.*, vol. 21, no. 1, pp. 118–121, Jun. 2014.
- [24] J. Li and P. Stoica, *MIMO Radar Signal Processing*. John Wiley & Sons, 2008.
- [25] K.-Y. Wang, A. M.-C. So, T.-H. Chang, W.-K. Ma, and C.-Y. Chi, "Outage constrained robust transmit optimization for multiuser MISO downlinks: Tractable approximations by conic optimization," *IEEE Trans. Signal Process.*, vol. 62, no. 21, pp. 5690–5705, Nov. 2014.
- [26] M. Grant and S. Boyd, "CVX: Matlab software for disciplined convex programming, version 2.1," Mar. 2014. [Online]. Available: <http://cvxr.com/cvx>
- [27] S. Ma, M. Hong, E. Song, X. Wang, and D. Sun, "Outage constrained robust secure transmission for MISO wiretap channels," *IEEE Trans. Wireless Commun.*, vol. 13, no. 10, pp. 5558–5570, Oct. 2014.
- [28] R. A. Horn and C. R. Johnson, *Matrix Analysis*. Cambridge university press, 2012.